

Design of Fault Tolerant Controller for Nonlinear Missile Autopilot

May 17, 2014

A Project Report

submitted by

Sreedhar Patnaik Dabbiru

Roll No. EE12M098

in partial fulfilment of the requirements
for the award of the degree of

MASTER OF TECHNOLOGY



Department of Electrical Engineering
Indian Institute of Technology Madras
May 2014

Thesis Certificate

This is to certify that the thesis titled **Design of Fault Tolerant Controller for Nonlinear Missile Autopilot**, submitted by **Sreedhar Patnaik Dabbiru**, to the Indian Institute of Technology, Madras for the award of the degree of MASTER OF TECHNOLOGY, is a bonafide record of the research work done by him under my supervision. The contents of this thesis, in full or in parts, have not been submitted to any other Institute or University for the award of any degree or diploma.

Dr. Ramkrishna Pasumarthu
Assistant Professor
(Research Guide)
Dept. of Electrical Engineering
I.I.T, Madras
Chennai-600036.
Date: 15th May, 2014

Acknowledgements

I take this opportunity to express my gratitude to my guide **Dr. Ramkrishna Pasumorthy**, for his exemplary guidance, monitoring and constructive suggestions throughout the course of this project. He always made sure that everything that is necessary for the project to be it equipment or knowledge was readily available. His sense of timing and his vast area of expertise have inspired me in so many ways. It has been wonderful experience, working under him.

I would like to thank **Dr. Arun Mahindrakar**, for his valuable feedback and innovative thoughts, a number of times during the course of the project. His expertise on *A Two-Time Scale Redesign for Robust Stabilization and Performance Recovery of Uncertain NonLinear systems* has inspired me to implement, a fraction of the same in my project.

I would also like to extend my thanks to all my senior colleagues from my sponsored organization viz. Defence Research and Development Organization, who shared the mission critical data to complete this project and also research scholars from control lab, I.I.T Madras, who helped me constantly giving their valuable feedback.

Sreedhar patnaik Dabbiru

Abstract

The motivation for studying Fault Tolerant Controller design for nonlinear autopilot arises from greater demand for production of highly reliable modern defence systems. Such conditions increase the possibility of system faults, which are characterized by critical and un-predictable changes in system dynamics. A Fault Tolerant Control (FTC) system is capable both of automatically compensating for faults and of maintaining the performance of controlled system, at some acceptable level even in the presence of faults.

According to the reliability study conducted by the US office of the secretary of Defence, about 80% of flight incidents are due to faults affecting propulsion, flight control sensors and actuators. Classically hardware redundancy (multiple actuators and sensors with the same function) and simple threshold to address the faults. Even if these techniques widespread in the defence and aerospace industry the additional costs and weights they imply are an impediment to autonomy especially for autonomous defence endgame.

In this project we propose a robust redesign technique which recovers the trajectories of nominal control design for 6 DOF nonlinear missile autopilot, in the presence of nonlinear faults exist in the pitch & yaw actuator input channels. We designed a high gain filter and employ the fast variables arising this filter in the feedback control law to cancel the the effect of faults and uncertainties in the plant. In the presence of a fault, the proposed controller guarantees the boundedness of all the system signals and output tracking error converges to neighborhood of zero.

Index Terms:- Fault Tolerant Controller, Nonlinear Autopilot, Actuator Faults, Pitch, Yaw, 6-DOF, High gain filter and output tracking error

Table of Contents

Acknowledgements	03
Abstract	04
List of Figures	08
List of Tables	10
List of Symbols	11
1. Introduction	13
1.1 Motivation	13
1.2 Literature Survey	16
1.2.1 Feedback Linearization based controller	16
1.2.2 Gain scheduled based controller	17
1.2.3 Sliding Mode controller	18
1.2.4 Model based Adaptive controller	18
1.2.5 Other approaches	18
1.3 Organization of the thesis	19
2. Theoretical Background	20
2.1 Two-Time Scale redesign technique	20
2.2 Time Scale separation & Backstepping techniques	24
3. Missile Basics	26
3.1 Missile Classification	26
3.2 Missile Subsystems	27

3.3	Missile Control	30
3.3.1	Aerodynamic	30
3.3.2	Jet reaction forces	30
3.4	Missile mathematical model	30
3.4.1	Frames of reference	31
3.4.2	Coordinate transformation between different frames	33
3.4.3	Aerodynamic nomenclature	34
3.4.4	6 DOF State space model in fin frame	35
3.4.5	Input to dynamical 6 DOF model	37
4.	Controller Design	44
4.1	Objective	44
4.2	Uncertain nonlinear missile dynamical model	44
4.3	Design of FTC	45
4.3.1	Design of nominal controller $u_{nom}(x)$	47
4.3.2	Design of desired controller $u_{des}(x)$	55
4.4	Input data for FTC	56
5.	Performance of Controller	58
5.1	Simulation platform and input data	58
5.2	Simulation results	59
5.2.1	Performance comparison for case study #1	59
5.2.2	Performance comparison for case study #2	67

6. Conclusion & Future Directions	75
6.1 Conclusion	75
6.2 Future directions	76
A. Stability Analysis of Uncertain Nonlinear System	78
B. Stability Analysis NDI Controller using Time Scale Separation	80
C. Theory of Feedback Linearization	83
Bibliography	88

List of Figures

- Fig 3.1: Basic Subsystems of Missile
- Fig 3.2: Block diagram of classical Lateral Autopilot
- Fig 3.3: Representation of Missile axis nomenclature and sign convention
- Fig 3.4: Aerodynamic force components along B-frame and W-frame
- Fig 3.5 : Fin Deflections
- Fig 4.1: Two-Time Scale Separation Autopilot Configuration
- Fig 4.2: Control structure of Nonlinear Outer Loop design
- Fig 5.1: Comparative tracking performance of Latex Pitch command and pitch rate(Case-1)
- Fig 5.2: Comparative tracking performance of Latex Yaw command and Yaw rate (Case-1)
- Fig 5.3 : Comparative tracking performance of Roll demand (Case-1)
- Fig 5.4 : Comparative fin deflection time profiles (Case-1)
- Fig 5.5 : Comparative performance of Pitch & Yaw deflection (δ_p δ_y) time profiles (Case-1)
- Fig 5.6 : Comparve trackig performance of Roll rate (p_f) and Roll deflection (δ_r) for Case-1
- Fig 5.7 : Comparative control law (δ_r , δ_p , δ_y) time profiles (Case-1)
- Fig 5.8 : Comparative performance of Angle-of-Attack & Roll Orientation time profiles (Case-1)
- Fig 5.9: Comparative tracking performance of Latex Pitch command and pitch rate(Case-2)
- Fig 5.10: Comparative tracking performance of Latex Yaw command and Yaw rate (Case-2)

Fig 5.11 : Comparative tracking performance of Roll demand (Case-2)

Fig 5.12 : Comparative fin deflection time profiles (Case-2)

Fig 5.13 : Comparative performance of Pitch & Yaw deflection ($\delta_p \delta_y$) time profiles (Case-2)

Fig 5.14 : Comparative tracking performance of Roll rate (p_f) and Roll deflection (δ_r) for Case-2

Fig 5.15 : Comparative control law ($\delta_r, \delta_p, \delta_y$) time profiles (Case-2)

Fig 5.16 : Comparative performance of Angle-of-Attack & Roll Orientation time profiles (Case-2)

List of Tables

Table 3.1 : Initial Euler Angles

Table 4.1: Autopilot demand at different time zones for case study-1

Table 4.2: Autopilot demand at different time zones for case study-2

List of Symbols

α	Angle of attack in <i>rad</i>
β	Side slip angle in <i>rad</i>
ϕ_a	Maneuver plane roll orientation in <i>rad</i>
g	Accelaration due to gravity $9.81 \frac{m}{s^2}$
$\delta_p, \delta_y, \delta_r$	Control Deflections in Pitch, Yaw and Roll respectively in <i>rad</i>
δ_1, δ_3	Control Deflections for Fin-1 and Fin-3 in <i>rad</i>
δ_2, δ_4	Control Deflections for Fin-2 and Fin-4 in <i>rad</i>
g_x, g_y, g_z	Gravity components in Fin frame along x, y and z directions respectively in $\frac{m}{s^2}$
I_{xx}, I_{yy}, I_{zz}	Moment of Inertia of the missile w.r.t x, y and z directions respectively in $\frac{kg}{m^2}$
p, q, r	Angular velocities of the missile around x, y and z axis respectively in $\frac{rad}{s^2}$
u, v, w	Linear velocities of the missile in x, y and z axis respectively in $\frac{m}{s}$
m	Mass of the missile in <i>kg</i>
Q	Dynamic Presssure of missile in <i>Pascal</i>
S	Surface Area of the missile in m^2
d	Effective diameter of the missile in <i>m</i>
T_x, T_y, T_z	Thrust components along x, y and z directions respectively in <i>Newton</i>
M, V_T	Mach Number and Resultant velocity along trajectory in $\frac{m}{s}$
f_z, f_y	Lateral accelerations (Latax) along z and y axis respectively in $\frac{m}{s^2}$
C_x, C_S, C_N	Drag, Side force and Normal force Coefficients in Body frame
C_D, C_y, C_L	Drag, Side force and Lift Coefficients in Fin frame
C_l, C_m, C_n	Rolling moment, Pitching moment and Yawing moment coefficients respectively
$C_l^{\delta_r}, C_m^{\delta_p}, C_n^{\delta_y}$	Moment Coefficients due to Roll, Pitch and Yaw deflections respectively

C_l^p, C_m^q, C_n^r	Damping Coefficients
$C_y^{\dot{\alpha}}, C_y^{\dot{\beta}}$	Force Coefficients due to derivatives of angle of attack and side slip angles
$C_m^{\dot{\alpha}}, C_n^{\dot{\beta}}$	Moment Coefficients due to derivatives of angle of attack and side slip angles
C_L^q, C_y^r	Cross coupling Force Coefficients due to Pitch and Yaw rates
δ_{rBS}	Roll deflection control law derived from back stepping method

Suffixes

f	Fin frame, Fast variable (context dependent)
s	Slow variable
b	Body frame
w	Wind / Velocity frame

Acronyms

FTC	Fault Tolerant Controller
LTI	Linear Time Invariant
LTV	Linear Time Varying
DOF	Degrees Of Freedom
SMC	Sliding Mode Control
SPC	Singular Perturbation Control
NDI	Nonlinear Dynamic Inversion
FL	Feedback Linearization
FV	Flight Vehicle
LPV	Linear Parameter Varying
ISS	Input to State Stable
STT	Skid-To-Turn
BTT	Bank-To-Turn
OBC	On Board Computer

Chapter1

Introduction

1.1 Motivation

The actuator mechanism which is the bridge between the controller and the component, plays an important role in the nonlinear missile system. The actuator mechanism fault has much effect on the whole missile system performance, even will cause the system paralysis and casualties. The actuator mechanism fault is always considered as the input type fault. So it is nessassery to design a fault tolerant controller which compensates for the faults. The objective of the controller, should guarantees the boundedness of all the system signals until the fault is cleared.

And classically missile autopilots are designed using linear control approaches. Linear autopilot is designed using linearized plant model on a fixed set of operating points. Such methods lead to design of Linear Time Invariant (LTI) controllers for the LTI systems. Operating points are in general defined by the triplet (Mach Number, Altitude and Angle of Attack), which are considered as slowly varying parameters. Interpolation techniques may then be used to connect local regions around these operating points.

The basic requirement for an autopilot are as follows

1. To obtain fast response satisfying subsystem constraint because of short amount of time involved in the endgame.
2. To obtain minimum steady state error as missile has to achive lowest possible *miss-distance*.
3. Robustness of model uncertainties and decoupling between longitudinal and lateral motion are important in order for the missile to achive its objective in the physical environment.

The highly nonlinear nature of missile dynamics, due to the severe kinematic and

inertial coupling of the missile airframe as well as the missile aerodynamics, has been a challenge to the autopilot design that is required to have the satisfactory performance for all flight conditions in all probable engagement scenarios.

In the last decade, the design of missile autopilot has been extensively studied using modern gain scheduling techniques and robust control. These methods are also based on local linearization. Modern day interceptor missiles are designed with high maneuverabilities to tackle highly agile and stealth target. High angle of attack operating region becomes imminent, resulting high cross coupling of lateral and longitudinal plane. Linear autopilot fails to address issue of cross coupling, as fundamental assumption of design of linear autopilot is decoupling of longitudinal and lateral motion.

To overcome these limitations, in last decade design of flight vehicle autopilots has been extensively studied using modern control design paradigms such as, robust control, feedback linearization, sliding mode control (SMC), singular perturbation control (SPC) etc. In this thesis we used a nonlinear multivariable approach to the design of an autopilot which includes pitch, roll and yaw coupling in design to overcome the difficulties associated with linear design.

Nonlinear Dynamic Inversion (NDI), also called Feedback Linearization (FL), is a control strategy that uses the model of a system to control it and through that eliminates the need for gain scheduling and improve performance. NDI using Time scale separation and SPC has been studied initially by Menon et al.[15] for designing nonlinear controller for aircraft and FV. In their research, they separated the whole dynamics into fast and slow dynamics according to the time response of the dynamics with respect to the input variables. Time scale separation exists in many aerodynamic systems and is applied to NDI flight control. Although the whole system is of nonminimum phase, each the fast and slow dynamics, according to the time response w.r.t the input variables, are of minimum phase. Thus each separated dynamics can be controlled by the FL technique. That is, the outer loop inversion

controller uses the states of the fast dynamics such as the body rates to control those of slow dynamics, and the inner loop inversion controller uses the fin deflections to control the state of the fast dynamics.

The roll autopilot design is very challenging because of roll uncertainties in roll aerodynamic coefficient, unmodelled dynamics, cross coupling, external disturbances, wing/fin and thrust misalignments, low roll moment of inertia, centre of gravity(CG) offset and measurement inaccuracies. Nonlinear controller design using backstepping is a viable alternative to FL technique. With backstepping, system nonlinearities do not have to be cancelled in the control law. How to deal with nonlinearities instead becomes a designer's choice. If a nonlinearity acts stabilizing, and thus in a sense is useful, it may be retained in the closed loop system. This leads to robustness to model errors and less control effort may be needed to control the system.

So, we are motivated to study a Two-Time scale redesign technique for robust stabilization and performance recovery of uncertain nonlinear system under faults. Here we proposed a new design which recovers the trajectories of a nominal control design in the presence of input faults. We designed a high-gain filter and employ the fast variables arising this filter in the feedback control law to cancel the effect of uncertainties in the plant.

The following activities are carried out in this thesis

- 1) Under nominal controller design, Pitch & Yaw autopilots are carried out using NDI with time scale separation technique and for Roll autopilot, nonlinear backstepping technique is used.
- 2) A Two-Time scale redesign technique is used to design a closed loop controller in the presence of actuator input faults.

1.2 Literature Survey

During last decade, a significant research effort has been contributed in the area of nonlinear missile autopilot design. The nonlinear design approaches found during survey are briefly classified into following methods

1. Feedback linearization based controller
2. Modern gain scheduled based controller
3. Sliding mode controller
4. Model based adaptive controller
5. Other approaches

1.2.1 Feedback linearization based controller

Feedback linearization[28] deals with techniques for transforming original system models into equivalent models of a simpler form. The basic idea is, first to transform a nonlinear system into a *fully* or *partial* linear system, and then use the well known and powerful linear design techniques to complete the control design. Nonlinear controllers based on Input-Output feedback linearization of the missile dynamics have a major advantage to linearize and decouple MIMO nonlinear systems. This technique can also be used as model simplifying devices for robust and adaptive controllers. Background on the application of the feedback linearization technique to missile autopilot problem can be found in the following references.

Devaud E, Siguerdidjane H et al.[23], [20], [22] and [21] presented a three-axis STT missile autopilot design using classical time invariant control and static and dynamic approximate input-output linearizing feedback control.

Schumacher C and Khargonekar P.P [9] and [36] examined the closed loop stability of a BTT, air-to-air missile with a dynamic inversion controller using time scale separation. A new nonlinear control method (called θ - D) is used to design a full envelope, hybrid BTT/STT autopilot for airbreathing air-to-air missile in Xin Ming and Balakrishnan's paper [14].

Application of nonlinear dynamic inversion for designing flight control for super

maneuvering aircraft is presented by Snell S.A., Enns D. F et al. [37]. Dynamic inversion missile autopilot by use of backstepping is also demonstrated by Steinicke A. and Michalka G [48].

Menon P.K., Tahk M. and Briggs M [38] presented the linearizing transformation technique to the autopilot design of air-to-air missile systems. The basic idea of this paper is to transform the nonlinear time varying control problems to time invariant problems there by simplifying the control design.

But the feedback linearization method has number of important limitations

1. It can't used for all nonlinear systems
2. The full state information is required
3. No robustness is guaranteed in the presence of parameter uncertainty or unmodeled dynamics.

1.2.2 Gain scheduled based controller

Gain scheduling is an attempt to apply the well developed linear control methodology to control of nonlinear systems[39]. The idea of gain scheduling is to select a number of operating points which cover the range of the system operation. Then at each of these points, the designer makes a LTI approximation to the plant dynamics and designs a linear controller for each linearized plant. Gain scheduling [41] is conceptually simple and indeed practically successful in missile applications [40].

Goshal T. K., and Das G. et al. [49] and Rugh W.J. and Jackson P. B [50] presented the three lateral loop autopilot design methodology and it's application in missile dynamics.

The main problem with gain scheduling is that it does not have any theoretical guarantee of stability in nonlinear operation, but uses some loose guidelines such as the *scheduling variable should change slowly* and the *scheduling variable should capture the plant's nonlinearities*. Another problem is the computational burden involved in a gain scheduling design due to the necessary of computing many linear controllers.

1.2.3 Sliding Mode Controller

The sliding mode control (SMC) technology [43] is an intuitive and simple robust control technique, addressing highly nonlinear systems with large modelling errors. The application of SMC for designing missile autopilot and guidance loops may be found in the following references.

Powly A.A. and Bhat M.S [42] presented a discrete variable structure controller for tracking the lateral command for a dual input air-to-air missile. The efficiency of the proposed controller is also brought out through simulation.

1.2.4 Model based adaptive controller

Adaptive control is an appealing approach to dealing with uncertain systems or time varying systems. Adaptive controllers, whether developed for linear systems or for nonlinear systems are inherently nonlinear. Systematic theories exist for the adaptive control of linear systems. Existing adaptive control techniques can also treat important class of nonlinear systems with measurable states and linearly parametrizable dynamics.

Applications of adaptive control and neural networks in aerospace autopilot design can be found in Rysdyk et al.[44]. This paper describes the combination of approximate feedback linearization with neural network augmentation to provide transport aircraft with a backup flight control system.

1.2.5 Literature related to other control approaches

Some more approaches to design the missile autopilots have been reported in [45] another different approach has been taken for autopilot design using Linear Parameter Varying (LPV) techniques. Here firstly the missile dynamics has been brought into an LPV form Via a state transformation rather than the usual coordinate transformation.

[46] and [47] present a missile autopilot design using Extended Mean Assignment (EMA) control technique for LTV systems. The EMA control technique is based on a new series D-eigen value (SD eigen value) concept in a way similar to the conventional pole placement design for LTI systems. The nonlinear dynamics of the missile is rendered into a linear one that is tractable by EMA control technique.

1.3 Organization of the thesis

Chapter1 describes the motivation of taking up this project

Chapter2 gives a theoretical background of Robust stabilization of uncertain nonlinear systems and brief history of nonlinear design techniques like Dynamic Inversion with Time-Scale Separation and Integrator Backstepping techniques.

Chapter3 provides the basics of the Missiles such as classification of Missiles, Missile subsystems like Guidance, Navigation and Autopilot control and Dynamic model of Missile.

Chapter4 explains the design aspects of the Fault Tolerant Controller with it's input data requirements.

Chapter5 gives the validation of the controller under the different case studies with it's performance exhibition.

Chapter6 gives the conclusion and then explains the future prospects for the project.

Chapter 2

Theoretical Background

2.1 Two-Time scale Redesign technique

Robust stabilization of uncertain nonlinear systems [1] has been a wide research interest over the past decades. Control redesigns via Lyapunov stability theory and Input-to-state stable (ISS) conditions to guarantee the stability of systems perturbed by unknown functions or parameters have been studied in great depth by numerous researchers. These include the robust backstepping design, adaptive backstepping and tuning functions, Geometric control designs and Sliding mode control.

The existing robust designs are motivated towards stabilization of the origin for the perturbed system and not account for the transient response of the redesigned closed loop system from the nominally controlled system. Depending on the desired precision and safety criticality of a system, changes in the transient response can be highly undesirable. To circumvent this problem, in this thesis we used a new redesign, in which we first design a high-gain filter and then use the fast variables arising from this filter in the nominal feedback control law in order to cancel the effect of the uncertain fault functions in the plant, so that after a fast transient the closed loop trajectories converge to the nominal trajectories.

We consider the system

$$\dot{x} = f(x) + g(x)(u + \delta(x)) \quad (2.1)$$

where $x \in \mathbb{R}^n$ is the *state*, $u \in \mathbb{R}^p$ is the *control input* and $f(x)$, $g(x)$ and $\delta(x)$ are sufficiently smooth functions of x . We assume that the functions $f(x)$, $g(x)$ are known while $\delta(x)$ is unknown *nonlinear, bounded uncertain/fault function* in x . To design a control input u which stabilizes the origin $x = 0$ of (2.1) despite the presence of $\delta(x)$, we make the following two assumptions.

Assumption 1: There exists a feedback control law $u = \alpha(x)$ such that the ori-

gin of the nominal closed loop system $\dot{x} = f(x) + g(x)\alpha(x)$ (2.2) is globally asymptotically stable, with a positive definite radially unbounded C^2 Lyapunov function $V(x)$ satisfying $\frac{\partial V}{\partial x}^T [f(x) + g(x)\alpha(x)] \leq -U(x) \quad \forall x \in R^n$ (2.3), where $U(x)$ is Positive Definite and possesses a positive definite Hessian $\frac{\partial^2 U}{\partial x^2}$ at $x = 0$.

Assumption 2: There exists a function $h(x) : R^n \rightarrow R^p$ such that the pxp matrix $G(x) := L_g h(x) = \frac{\partial h}{\partial x} g(x)$ is non singular for all x .

With this assumptions we note that the variable $y = h(x)$ satisfies

$$\dot{y} = L_f h(x) + G(x)(u + \delta(x)) \quad (2.4)$$

To estimate the unknown $\delta(x)$ we design a filter

$$\hat{y} = L_f h(x) + G(x)u - \frac{1}{\epsilon}(\hat{y} - y), \quad \hat{y}(0) = y(0) \quad (2.5)$$

where the parameter $\epsilon > 0$ will be selected. Then from (2.4) and (2.5),

$$\text{the variable} \quad l := \frac{\hat{y} - y}{\epsilon} \quad (2.6)$$

$$\text{satisfies} \quad \epsilon \dot{l} = -l - G(x)\delta(x), \quad l(0) = 0. \quad (2.7)$$

When ϵ is small, l evolves in the faster time scale than x , and reaches a small neighborhood of the manifold

$$l = -G(x)\delta(x) \quad (2.8)$$

Therefore, a plausible design for u to cancel the effect of $\delta(x)$ in (2.1) would be

$$u = \alpha(x) + G^{-1}(x)l \quad (2.9)$$

It is noted that the desired control law (Eqn 2.9) is a combination of Nominal control law and filter dynamics. So, In order to design a Fault Tolerant Controller, one has to design nominal controller using any suitable technique in conjunction with high-gain filter design.

2.2 Time Scale Separation & Back Stepping Techniques

Basic motivation of designing nonlinear autopilot for a high performance missile is to follow reference guidance generated latex commands with desired transient response and accuracy. Latex control is always desirable as this controls the angle of attack and there by controls plant effectively in the presence of high magnitude

and low frequency disturbance in the form of wind and gust. Most of missiles are Skid-To-Turn (STT) type to have accurate 2-plane guidance. Unfortunately fin/tail controlled STT missile suffers from non-minimum phase zero apart from more coupling terms compared to Bank-To-Turn (BTT) missiles.

In nonlinear framework this problem is solved using two types of approaches:

1) To control a output variable which is combination of angle of attack and latex. This redefined variable does not possess nonminimum phase characterestic and can be controlled but transient response is poor.

2) Using Dynamic Inversion with Time Scale Separation controller using time scale separation [15] properties of missile.

Model inversion control using time-scale separation is studied using singular perturbation and applied by separating the whole dynamics into fast and slow dynamics, according to the time response of the dynamics with respect to the input variables [2]. Here the fast dynamics are assumed to go to steady state quickly, and thus the reduced system can be obtained. Actually Time Scale Separation exists in many aerodynamic systems and is applied to model inversion flight control. Although the whole system is of nonminimum phase, each fast and slow dynamics, separated from the original dynamics according to the time response with respect to the input variables, are of minimum phase.

Thus, each separated dynamics can be controlled by the feedback linearization technique. That is the outer loop inversion controller uses the states of the fast dynamics to control those of the slow dynamics , and the inner loop inversion controller uses the control fin deflection to control the states of fast dynamics. The dependencies can be symbololically represented using the following expressions:

$$\delta_r \Rightarrow p \Rightarrow \phi \tag{2.10}$$

$$\delta_p \Rightarrow q \Rightarrow \alpha \Rightarrow a_z \tag{2.11}$$

$$\delta_y \Rightarrow r \Rightarrow \beta \Rightarrow a_y \tag{2.12}$$

Eqn (2.10-2.12) state that the roll, pitch and yaw fin deflections influence the body rates, which in turn influence the roll attitude, angle of attack and angle of side slip. The angle of attack and angle of side slip influence the pitch and yaw latex.

2.2.1 Nonlinear Dynamic Inversion Controller with Time Scale Separation

The basic concept behind the Time Scale Separated NDI controller is to follow commanded input with desired fastness and accuracy when original plant can be thought of as one minimum phase fast subsystem and one minimum phase slow subsystem. This is achieved by inverting the governing equations of the individual subsystem dynamics based on measured states and input commands.

Let the nonlinear system along any pursuer interest axes like *Inertial, Local Vertical, Body, Wind and Fin frames* are represented by

$$\dot{x} = f(x) + g(x)u \quad (2.13)$$

Here state variables $x = [\phi \ \alpha \ \beta \ p \ q \ r]^T$

where $\phi \rightarrow$ Roll Orientation, $\alpha \rightarrow$ Angle of Attack, $\beta \rightarrow$ Side Slip Angle, $p \rightarrow$ Roll Rate, $q \rightarrow$ Pitch Rate, $r \rightarrow$ Yaw Rate.

Using time scale separation, fast and slow state dynamics can be separated as

$$\begin{aligned} \dot{x}_s &= f_s(x_s) + G_s(x_s)x_f & y_s &= h_s(x_s, x_f) \\ \dot{x}_f &= f_f(x_f) + G_f(x_f)u & y &= h_f(x_f, u) \end{aligned} \quad (2.14)$$

Separating the state variable $x = (x_s, x_f)^T$ as slow and fast variables respectively and defining the slow variables $x_s = (\phi, \alpha, \beta)^T$ and fast variables $x_f = (p, q, r)^T$.

- The measurements of slow variable dynamics are on-board accelerometer outputs i.e $y_s = (\phi, a_y, a_z)^T$. Taking the derivative of the outputs

$$\dot{y}_s = \begin{pmatrix} \dot{\phi} \\ \dot{a}_y \\ \dot{a}_z \end{pmatrix} = \left(\frac{\partial h_s}{\partial x_s} \right) [f_s(x_s) + G(x_s)x_f] = \left(\frac{\partial h_s}{\partial x_s} \right) f_s(x_s) + \left(\frac{\partial h_s}{\partial x_s} \right) G(x_s)x_f = L_{f_s}h + \Delta x_f \quad (2.15)$$

from the fictitious input \dot{y}_s , extracting the *control law* as $u_s = x_f = -\Delta^{-1} [L_{f_s}h - \dot{y}_s]$ which asymptotically tracks the output y_s . Similarly for fast variable dynamics also.

2.2.2 Integrator Backstepping technique

Consider the nonlinear system [2]

$$\dot{x} = f(x) + g(x) \xi; \quad \dot{\xi} = u \quad (2.16)$$

Assumption:- \exists a state feedback control law $\xi = \phi(x)$ in which $\phi(0) = 0$ and a Lyapunov function $V_1(x) > 0$. Then $V_1(x)$ satisfies the following inequality

$$\dot{V}_1(x) = \left(\frac{\partial V_1}{\partial x}\right)^T \dot{x} = \left(\frac{\partial V_1}{\partial x}\right)^T [f(x) + g(x) \xi] \leq -V_a(x) \quad (2.17)$$

where $V_a(x) > 0$ (positive definite) and it has to be selected.

Observation:- When $x = 0$ $\xi(x) = \phi(0) = 0$. Then from Equation (2.16) $\dot{x}(0) = f(0) = 0$. But when $\xi \rightarrow 0$ $\dot{x} = f(x)$ and hence $x \neq 0$.

Hence let us add and subtract $g(x) \phi(x)$ in Equation (2.16) to obtain

$$\dot{x} = [f(x) + g(x)\phi(x)] + g(x)[\xi - \phi(x)] \quad (2.18)$$

Let $z \triangleq \xi - \phi(x)$ which generates the following system equations

$$\dot{x} = [f(x) + g(x)\phi(x)] + g(x)z; \quad \dot{z} = \dot{\xi} - \dot{\phi}(x) = u - \dot{\phi}(x); \quad \dot{\xi} = u \quad (2.19)$$

This change of variable is often called *backstepping* since it backsteps the control $-\phi(x)$ through the integrator. Since $f, g, \phi(x)$ are known, the derivative can be written as

$$\dot{\phi}(x) = \left(\frac{\partial \phi}{\partial x}\right)^T \dot{x} = \left(\frac{\partial \phi}{\partial x}\right)^T [f(x) + g(x) \xi] \quad (2.20)$$

Letting $v = u - \dot{\phi}(x)$ reduces our system to an equivalent system as

$$\dot{x} = [f(x) + g(x)\phi(x)] + g(x)z; \quad \dot{z} = v \quad (2.21)$$

This equation (Eqn 2.21) has the same form as the system we started (Eqn 2.16). This modularity property of backstepping will be exploited to stabilize the overall system.

Let us define a candidate Lyapunov function using Eqn (2.17) and Eqn (2.21)

$$V(x, z) = V_1(x) + \frac{1}{2} z^2 \quad (2.22)$$

Let us calculate derivative of Eqn (2.22) and by substitution of relevant terms of Eqn (2.17) and Eqn (2.21) we get

$$\dot{V}(x, z) = \dot{V}_1(x) + z \dot{z} = \left(\frac{\partial V_1}{\partial x}\right)^T [f(x) + g(x)\phi(x) + g(x)z] + z v \quad (2.23)$$

$$= \left(\frac{\partial V_1}{\partial x} \right)^T [f(x) + g(x)\phi(x)] + \left[\left(\frac{\partial V_1}{\partial x} \right)^T g(x) + v \right] z \leq -V_a(x) + \left[\left(\frac{\partial V_1}{\partial x} \right)^T g(x) + v \right] z$$

$$\text{Let us select } = - \left(\frac{\partial V_1}{\partial x} \right)^T g(x) - k_3 z - k_4 z^3 \quad (2.24)$$

Then from Eqn (2.23) gets reduced to $(V_a(x))$ is positive definite, $k_3 > 0, k_4 > 0$

$$\dot{V} \leq -V_a(x) - k_3 z^2 - k_4 z^4 < 0 \quad (2.25)$$

So the control can be defined as (Refer Eqn.2.19, Eqn.2.21)

$$u = \dot{\phi}(x) + v = \dot{\phi}(x) - \left(\frac{\partial V_1}{\partial x} \right)^T g(x) - k_3 z - k_4 z^3 \quad (k_3, k_4 > 0)$$

$$z = \xi - \phi(x) \quad (2.26)$$

$$\dot{\phi}(x) = \left(\frac{\partial \phi}{\partial x} \right)^T [f(x) + g(x)\xi]$$

Chapter 3

Missile Basics

A missile is a projectile that is, something thrown or otherwise propelled. The earliest form of missile was probably a stone that, when thrown forcefully through the air, would follow a balastic path. Adding gun power to a projectile, resulted in the rocket, the first powered but as yet unguided missile. Rockets was first invented in medieval China (Circa 1044 AD) but its first practical use for serious purpose other than entertainment took place in 1232 AD , by the Chinese against the Mongols at the Siege of Kai-Feng-Fue. There after from 1750 AD to 1799 AD Haider Ali and Tipu Sulatan perfected the rockets's use for military purpose very effectively using it in war against British colonial armies. It was not until the early 1900s that guided missile development was begun. In so far as the missile we know it today is concerned, the impetus came primarily from world war-II and in particular from German scientists. Immediately after world war there was a rapid growth in missile defence activity throughout the world. Although this work is concerned with a particular type of short range missile autopilot.

3.1 Missile Classification

Missiles can be classified mainly, according to the following design technologies, eventhough there are other subclasses.

- 1) **Tactical Vs Strategic**— Depends upon the type of guidance laws used.
- 2) **Short Range, Medium Range, Long Range, IRBM and ICBM**— Depends upon the horizontal distance travelled.
- 3) **SSM, SAM, ASM, SSM , Anti Tank and Cruise Missiles** —Depends upon type of launching environment.
- 4) **Sub Sonic, Super Sonic and Hyper Sonic Missiles**— Depends upon the Mach Number (M) of travelling speed.
- 5) **Depressive Vs Lofted Trajectory Missiles** — Depends upon the attained maximum height in the atmosphere.

3.2 Missile Subsystems

A missile consists of several subsystems to achieve its goal with minimum *miss distance*. The most closely related subsystems are shown in the block diagram Fig 3.1 which describe the principle function of each subsystem and list the principle elements of each.

3.2.1 Navigation

When missile is launched, its position, attitude, speed, acceleration and rotation are to be known. The navigation subsystem updates these variables during the flight. This is done by using the sensor data and strap down navigation algorithms. These variables are supplied to the guidance subsystems.

3.2.2 Guidance

The guidance subsystem computes the error between the missile's actual and desired courses, computes the corrections necessary to reduce or nullify the error according to a chosen guidance law, and gives commands to the autopilot to activate the controls to achieve the corrections. These commands may be Lateral accelerations (Latex), angular rates etc. The navigation system contains the sensors that provide the information on the missile's actual and desired trajectories, noise filters and a computer in guidance system (OBC) to process the information into the commands to the autopilot.

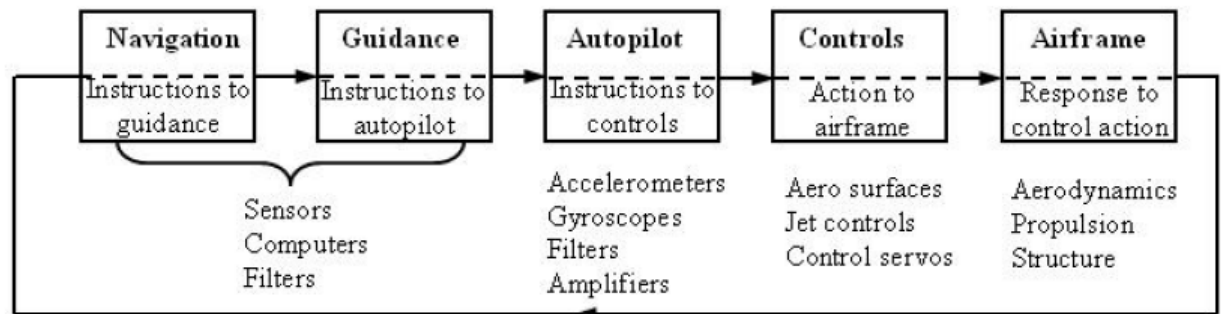


Fig 3.1 : Basic Subsystems of Missile

3.2.3 Autopilot

The autopilot receives the commands from the guidance computer and process them into commands to the controls such as deflections or rates of deflection of control surfaces or jet controls through action of servomechanisms. To provide the deflection at a desired rate, the servomechanism motors must contend with the inertia of the control device and the torque about itself. Since the autopilot will convert guidance commands of acceleration or angular rate into control commands, it must have a way to determine if the accelerations and angular rates provided by deflecting the controls are meeting the guidance commands. Thus this subsystem will have accelerometers for measuring the achieved accelerations and gyroscopes for measuring the angular positions or rates. Depending on where these measurements are placed, the autopilot may have to provide corrections to the instrument readings to obtain the true accelerations of the missile's center of gravity (CG) and true angular rates about the principle axes. Classically, the missile autopilot comprises the three independent autopilots, one for each lateral direction, namely Pitch and Yaw, and one for Roll.

3.2.3.1 Lateral Autopilot

The missile autopilot controls the acceleration normal to the missile body. In this case the autopilot structure is a *three-loop* topology using measurements from an *accelerometer* located ahead of the missile's centre of gravity and from a *rate gyro* to provide additional damping. Fig 3.2 shows the classical configuration of an autopilot. The controller gains are scheduled based on *Mach Number* and tuned for robust performance at an altitude of around 4000 mtrs (10000 ft) in general for small range surface-to-surface STT missiles. According to the Fig 3.2 there are three feedback loops are present.

Since control of acceleration is required, the outermost loop is closed by an accelerometer and have *lowest bandwidth* among the three loops. The *innermost rate-damping loop* is required to damp the response of bare airframe, which has an under-

damped resonance in the stable case. In addition the innermost rate-damping loop has *wide bandwidth* for damping the poles of airframe. The last one, known as *synthetic stability loop*, improves the high frequency poles of the autopilot if the airframe is stable and enables the autopilot to tolerate some instability of the airframe. Furthermore the synthetic stability loop in Fig 3.2 effectively feeds incremental pitch angle back to the fin servos, thereby moving the autopilot closedloop poles, corresponding to the bare airframe poles. Three important parameters of three-loop autopilot i.e system damping, time constant of desired latex demand transfer function $\frac{f_x}{f_y}$ and open loop crossover frequency of innermost loop need to be tightly controlled.

Controlling system damping ensures that guidance system is not sensitive to body rate coupling. Selecting and controlling system time constant to the specified value as per *guidance loop* requirement tightly, means that adequate performance in terms of *miss distance* can be achieved. Finally controlling cross over frequency means that we will have a robust design, which is not overly sensitive to un-modelled high frequency dynamics.

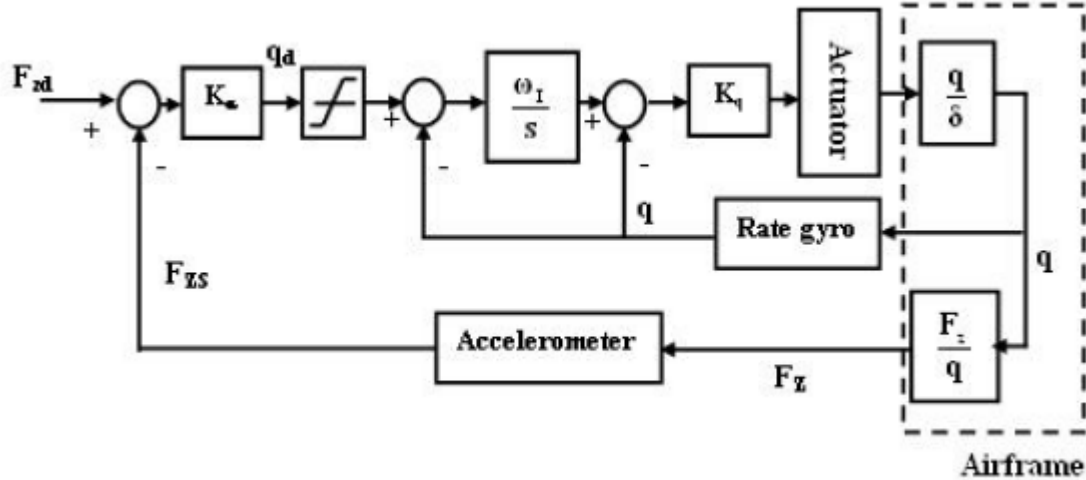


Fig 3.2 : Block diagram of classical Lateral Autopilot

3.2.3.2 Roll Autopilot

The basic function of *Roll Autopilot* is to make the missile *roll stabilized*, that is to provide missile stabilization of roll attitude about the longitudinal axis. This is accomplished by sensing *roll rate*, and using the fins(or wings) deflection by an amount sufficient to *counteract roll disturbances*. Moreover, the response of the system must be sufficiently fast to prevent the accumulation of significant roll angles.

3.3 Missile Control

The choice of the control system will depend on the use of the missile, flight path and the height at which it will operate. There are two main control systems used

3.3.1 Aerodynamic

Aerodynamic change of flight path is obtained by using a wing at incidence to the direction of flight. The wing is set at incident in one of the two ways:

- By using a rotatory wing
- By using a fixed wing, but movable control surface to set the whole missile at incidence. The control surfaces may be at the front or rear of the missile.

3.3.2 Jet reaction forces

Change of flight path by jet reaction forces is achieved in one of the two ways:

- By altering the direction of thrust of the propulsion unit, either by swivelling the whole unit, or by deflecting the gas stream by vanes or similar devices.
- By the use of separate auxiliary jet reaction units.

3.4 Missile Mathematical Model

The missile 6 DOF model will consists of 19 differential equations. This includes aero data model, thrust model, jet vane model apart from dynamics of

- Missile Velocities (Fin frame)
- Missile Positions (Launcher frame)

- Missile Body rates (Fin frame)
- Euler Angles (Launcher to Body frame)
- Inertial Velocities (Launcher frame)

The frames of reference and sign convention employed are described in the following section.

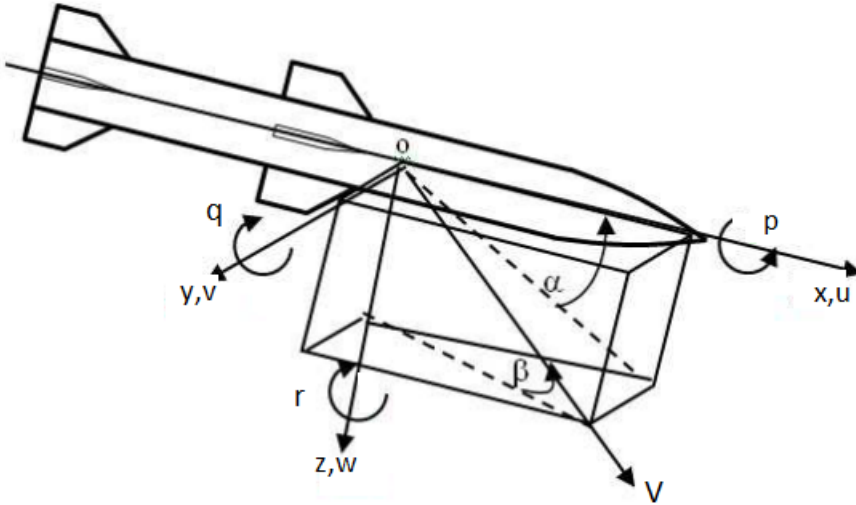


Fig 3.3 : Representation of Missile axis nomenclature and sign convention

3.4.1 Frames of reference

The following frames of reference (with it's suffix in brackets) are used in the present module.

1. Launcher Frame(i)
2. Body frame(b)
3. Stability axis frame(s)
4. Wind axis frame(w)
5. Fin axis frame(f)

The sign convention followed for the above frames are such that, forces are considered positive if they act along the positive axis direction and moments are taken to be positive if the rotation is anti-clockwise as seen from the tip to root of the axis.

- **Local Vertical or Launcher Frame**

This is a frame on the surface of the earth, whose origin coincides with the missile's center of gravity just before launch and axes directions are: x-axis vertically up, y-axis towards east and z-axis in the north direction. Hence this frame of reference is also called Launcher fixed VEN (Vertical-East-North) frame.

This frame is assumed to be inertial for the missile motion and so it is important for the computation of guidance parameters on the basis of missile trajectory in this frame.

- **Body frame**

The Body frame considered for the present module is the frame whose origin is located at the center of gravity and x-axis parallel to the geometric axis of symmetry of the missile and y-axis in the starboard direction while z-direction completes the right handed triad. The y-z axis is such that the fins are cross to these axis directions.

This frame is quite important for defining the missile dynamic equations of motion and evaluating certain important aerodynamic parameters.

- **Stability axis frame**

Stability axis frame is obtained from body axis frame after the rotation of x-z axis of body frame by an angle of attack (α). This frame is generally used for analysing the effect of perturbations from steady-state flight.

- **Wind axis**

Wind axis frame is obtained from Stability axis frame after the rotation of x-y axis of Stability frame by an angle of Side slip (β). It is worth noting that *Lift*, *Drag* and *Cross-wind* are naturally defined with wind axes frame.

- **Fin axis frame**

This frame have all the characteristics common to the body frame, except that here the y and z directions are along the missile fins. Here this frame is achieved by a $\frac{\pi}{4}$ rotation of body frame along positive x-axis in right handed manner. This frame is quite important from the point of view of deflections given to fins.

3.4.2 Coordinate Transformation between different frames

Because there is often a need to transform the missile velocities, accelerations or other vector quantities from one frame to another. The transformations between these frames are important and are used extensively in the guidance of the missile. So the following transformation matrices have been obtained.

- **Transformation matrix from Launcher frame to Body frame (Euler Angles)**

At time of launch, the missile body axis (x_b, y_b, z_b) are oriented with respect to launcher frame (x_L, y_L, z_L) at Euler angles (ϕ, θ, ψ) , where order of rotation is $\phi \rightarrow \psi \rightarrow \theta$. For these Euler angles the transformation matrix is given by

$$T_{LV2B} = \begin{bmatrix} \cos\theta & 0 & -\sin\theta \\ 0 & 1 & 0 \\ \sin\theta & 0 & \cos\theta \end{bmatrix} \begin{bmatrix} \cos\psi & \sin\psi & 0 \\ -\sin\psi & \cos\psi & 0 \\ 0 & 0 & 1 \end{bmatrix} \begin{bmatrix} 1 & 0 & 0 \\ 0 & \cos\phi & \sin\phi \\ 0 & -\sin\phi & \cos\phi \end{bmatrix} \quad (3.1)$$

- **Transformation matrix from Body frame to Wind frame**

Since wind frame is obtained by rotating body axis frame first by an amount of angle-of-attack (α) about it's y-axis (Resultant known as Stability axis) and then rotating by angle of side slip (β) about z-axis of stability axis.

Therefore the transformation matrix is given by

$$T_{B2W} = \begin{bmatrix} \cos\beta & \sin\beta & 0 \\ -\sin\beta & \cos\beta & 0 \\ 0 & 0 & 1 \end{bmatrix} \begin{bmatrix} \cos\alpha & 0 & \sin\alpha \\ 0 & 1 & 0 \\ -\sin\alpha & 0 & \cos\alpha \end{bmatrix} \quad (3.2)$$

- **Transformation matrix from Body frame to Fin frame**

Since the fin frame is achieved by a rotation of body frame about positive x-axis by an angle of 45° in right handed manner. Hence the transformation matrix from the body frame to fin frame is given by

$$T_{B2FIN} = \begin{bmatrix} 1 & 0 & 0 \\ 0 & \cos\left(\frac{\pi}{4}\right) & \sin\left(\frac{\pi}{4}\right) \\ 0 & -\sin\left(\frac{\pi}{4}\right) & \cos\left(\frac{\pi}{4}\right) \end{bmatrix} \quad (3.3)$$

3.4.3 Aerodynamic Nomenclature

The forces acting on the missile in flight, consists of *Aerodynamic*, *Thrust* and *Gravitational forces*. These forces are can be resolved along an axis system fixed to the missile's center of gravity (CG). The force components denoted as X,Y and Z; T_x , T_y and T_z ; and W_x , W_y and W_z are the aerodynamic, thrust and gravitational force components along x, y and z axes respectively.

The aerodynamic forces are defined in terms of *Dimensionless coefficients*, the flight *Dynamic pressure* (Q) and a *reference area* (S) as follows.

With respect to missile body axis

$$\begin{aligned} X &= C_x Q S & \text{Axial force} \\ Y &= C_y Q S & \text{Side force} \\ Z &= C_z Q S & \text{Normal force} \end{aligned} \tag{3.4}$$

With respect to the wind/velocity axis

$$\begin{aligned} D &= C_D Q S & \text{Drag force} \\ Y &= C_y Q S & \text{Side force} \\ Z &= C_L Q S & \text{Lift} \end{aligned} \tag{3.5}$$

In a similar manner, the moments on the missile can be divided into moments created by the aerodynamic load distribution and the thrust force not acting through the center of gravity(CG). The components of the aerodynamic moment are also expressed in terms of dimensionless coefficients, flight dynamic pressure (q), reference area (S) and characteristic length (l) as follows

$$\begin{aligned} L &= C_l Q S l & \text{Rolling moment} \\ M &= C_m Q S l & \text{Pitching moment} \\ N &= C_n Q S l & \text{Yawing moment} \end{aligned} \tag{3.6}$$

The aerodynamic coefficients $C_x, C_y, C_z, C_D, C_L, C_l, C_m$ and C_n primarily are functions of the Mach number (M), Reynolds number (Re), Angle-of-Attack (α) , Side slip angle (β) and control deflection (δ); they are the secondary functions of the time rate of change of angle of attack and side slip, and the angular velocity of the

missile.

The functional dependance of aerodynamic coefficient is represented as

$$C_* = C_*(M, \alpha, \beta, \dot{\alpha}, \dot{\beta}, \delta) \quad (3.7)$$

(* may represents $N, S, x, y, L, D, l, m, n$ and δ etc.)

The derivative of equation (3.7) is computed for general coefficient case is illustrated below

$$\begin{aligned} dC_* &= \left(\frac{\partial C_*}{\partial M}\right) dM + \left(\frac{\partial C_*}{\partial \alpha}\right) d\alpha + \left(\frac{\partial C_*}{\partial \beta}\right) d\beta + \left(\frac{\partial C_*}{\partial \delta}\right) d\delta + \dots\dots\dots H.O.T \\ &= C_*^M dM + C_*^\alpha d\alpha + C_*^\beta d\beta + C_*^\delta d\delta + \dots\dots\dots \end{aligned} \quad (3.8)$$

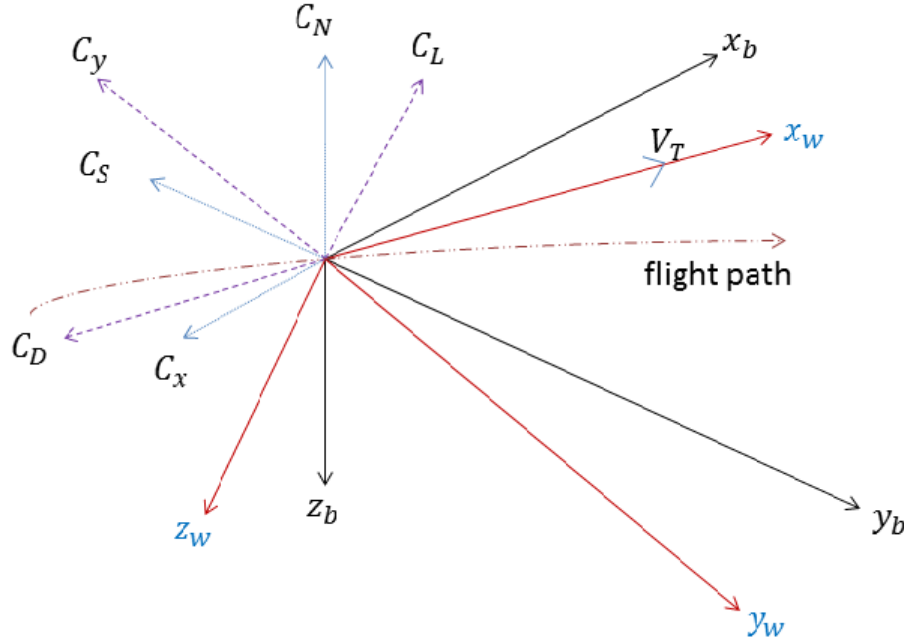


Fig 3.4: Aerodynamic force components along B-frame and W-frame

3.4.4 6 DOF State Space model in Fin frame

The nonlinear differential equations for the missile model written in the Fin frame are given as [51]

$$\begin{aligned}
\dot{u}_f &= r_f v_f - q_f w_f + \frac{1}{m} [T_x - QSC_D^0] - g_x \\
\dot{v}_f &= p_f v_f - r_f u_f + \frac{1}{m} \left[T_y + QS \left\{ C_{NB} + C_n^{\delta_y} \delta_y + \frac{d}{2V_T} \left(-C_y^{\dot{\beta}} \dot{\beta} + C_y^{r_f} r_f \right) \right\} \right] - g_y \\
\dot{w}_f &= q_f u_f - p_f v_f + \frac{1}{m} \left[T_z + QS \left\{ C_{NA} - C_m^{\delta_p} \delta_p + \frac{d}{2V_T} \left(-C_y^{\dot{\alpha}_f} \dot{\alpha}_f + C_L^{q_f} q_f \right) \right\} \right] - g_z \\
\dot{p}_f &= \frac{1}{I_{xx}} \left[-I_{xx} p_f + M_x - (I_{zz} - I_{yy}) q_f r_f + QSd \left(C_l - C_l^{\delta_r} \delta_r + \frac{d}{2V_T} C_l^{p_f} p_f \right) \right] \\
\dot{q}_f &= \frac{1}{I_{yy}} \left[-I_{yy} q_f + M_y - (I_{xx} - I_{zz}) p_f r_f + QSd \left(C_{MA} - C_m^{\delta_p} \delta_p \right) + QSd \frac{d}{2V_T} \left(C_m^{q_f} q_f + C_m^{\dot{\alpha}_f} \dot{\alpha}_f \right) \right] \\
\dot{r}_f &= \frac{1}{I_{zz}} \left[-I_{zz} r_f + M_z - (I_{yy} - I_{xx}) p_f q_f + QSd \left(C_{MB} - C_n^{\delta_y} \delta_y \right) + QSd \frac{d}{2V_T} \left(C_n^{r_f} r_f + C_n^{\dot{\beta}_f} \dot{\beta}_f \right) \right]
\end{aligned} \tag{3.9}$$

$$\text{Where } \begin{bmatrix} g_x & g_y & g_z \end{bmatrix}^T = \begin{bmatrix} g \sin \theta & -\frac{g}{\sqrt{2}} \cos \theta (\sin \phi + \cos \phi) & \frac{g}{\sqrt{2}} \cos \theta (\sin \phi - \cos \phi) \end{bmatrix}^T$$

Here the state variables (u_f, v_f, w_f) are forward velocities and (p_f, q_f, r_f) are body rates of missile w.r.t fin frame. These state variables can be transformed into user interested frame by it's equivalent Transformation.

C_{NB} and C_{NA} are resultant aero force coefficients in v_f and w_f axis respectively. The corresponding resultant moment coefficients are C_{MB} and C_{NA} . The resultant coefficients, C_{NB} , C_{NA} , C_{MB} and C_{MA} are obtained as below from C_N , C_S , C_m and C_n which are wind tunnel data reference to relative wind axis.

$$\begin{aligned}
C_{NA} &= -C_N \cos \phi_a - C_S \sin \phi_a \\
C_{NB} &= -C_N \sin \phi_a + C_S \cos \phi_a \\
C_{MA} &= C_m \cos \phi_a + C_n \sin \phi_a \\
C_{NA} &= -C_m \sin \phi_a + C_n \cos \phi_a
\end{aligned}$$

The required state variables of interest, $(\phi_f, \alpha_f, \beta_f)$ are computed by following relationship

$$\begin{aligned}
\phi_f &= \tan^{-1} \left(\frac{\tan \beta_f}{\tan \alpha_f} \right) \\
\alpha_f &= \tan^{-1} \left(\frac{(w_f - U_{zf})}{(u_f - U_{xf})} \right)
\end{aligned} \tag{3.10}$$

$$\beta_f = \tan^{-1} \left(\frac{(v_f - U_{yf})}{(u_f - U_{xf})} \right)$$

where U_{xf}, U_{yf}, U_{zf} are the wind velocities in X, Y, Z directions respectively with reference to fin frame, and $(\delta_1, \delta_2, \delta_3, \delta_4)$ are individual fin deflections.

Now the state variables of interest are $x = (\phi_f, \alpha_f, \beta_f, p_f, q_f, r_f)^T$. The derivative of state variables ϕ_f, α_f and β_f are obtained by differentiating Eqn (3.10) and substituting the Eqn (3.9).

Now, the derivative of the state variables ϕ_f, α_f and β_f [8] are given below

$$\begin{aligned} \dot{\phi}_f &= p_f - (q_f \sin \phi_f + r_f \cos \phi_f) \cot \alpha_R + \frac{(a_y \cos \phi_f - a_z \sin \phi_f)}{V_T \sin \alpha_R} \\ \dot{\alpha}_f &= q_f - (p_f \cos \alpha_f + r_f \sin \alpha_f) \cos \alpha_f \tan \beta_f + \frac{(a_z \cos \alpha_f - a_x \sin \alpha_f) \cos \alpha_f}{\sqrt{1 + \tan^2 \alpha + \tan^2 \beta}} \\ \dot{\beta}_f &= -r_f + (p_f \cos \beta_f + q_f \sin \beta_f) \cos \beta_f \tan \alpha_f + \frac{(a_y \cos \beta_f - a_x \sin \beta_f) \cos \beta_f}{\sqrt{1 + \tan^2 \alpha + \tan^2 \beta}} \end{aligned} \quad (3.11)$$

Where $\alpha_R = \tan^{-1} \left(\sqrt{\tan^2 \alpha_f + \tan^2 \beta_f} \right)$ and (a_x, a_y, a_z) are accelerations in x, y and z directions respectively

3.4.5 Input to dynamical 6 DOF model

Launcher orientation angles:- Initial elevation (γ_{init}) and azimuth (ψ_{init}) angles of launch of missile are given by pre-launch computation algorithm (Ground guidance computation) for inclined launch. For vertical launch, these angles are fixed, $\gamma_{init} = 90^\circ$ and $\psi_{init} = 0^\circ$. With the help of these angles the orientation of the body frame with respect to launcher frame just before the launch is obtained. Hence the Euler angles just before the launch is obtained as below:

Inclined Launch	Vertical Launch
$\theta_i = -\left(\frac{\pi}{2} - \gamma_{init}\right)$	$\theta_i = 0$
$\phi_i = -\psi_{init}$	$\phi_i = 0$
$\psi_i = 0$	$\psi_i = 0$

Table-3.1: Initial Euler angles

These Euler angles are used in the calculation of Direction Cosine Matrix (DCM) as in Equation (3.1)

3.4.5.1 Fin deflections

The fin deflection corresponding to four fins of the missile are $\delta_1, \delta_2, \delta_3$ and δ_4 . Where (δ_1, δ_3) are deflections of Yaw plane and (δ_2, δ_4) are deflections of Pitch plane with respect to fin frame as shown in Fig.3.5. Hence the effective Pitch, Yaw and Roll deflections in fin frame can be defined as below:

$$\begin{aligned}\delta_y &= \left(\frac{\delta_1 - \delta_3}{2.0} \right) \\ \delta_p &= \left(\frac{\delta_2 - \delta_4}{2.0} \right) \\ \delta_r &= \frac{1}{2} (\delta_1 + \delta_2 + \delta_3 + \delta_4)\end{aligned}\tag{3.12}$$

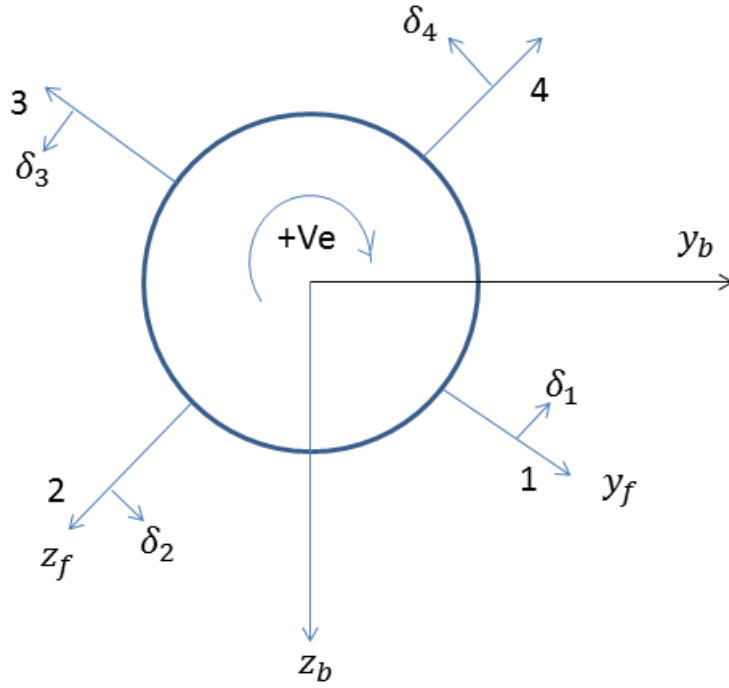


Fig 3.5 : Fin Deflections

3.4.5.2 Time and Time update

The 6 DOF differential equations are solved just after the launch of the missile and all these differential equations are coupled and the only independent variable is time. Hence this system of differential equations must be solved together, with the same time step at the same time. Hence two variables t_M and dt_M have been defined,

where t_M denotes missile flight time and dt_M denotes the step size.

Hence t_M is inilized with zero, just before the launch. And dt_M value is selected on the basis of fastest subsystem involved in the missile or the accuracy&speed requirements.

So t_M and dt_M are inilized as below:

$$t_M = 0$$

$$dt_M = 2.5 \text{ ms}$$

3.4.5.3 Inilization of velocity and height

The initial position & velocity of the missile (Position & Velocity at $t_M = 0$) are zero. Because at the time of launch the center of mass (C M) of the missile is co-incides with the origin of the coordinate system, so missile position is zero in all the coordinate frames defined earlier, at $t_M = 0$ and as missile is at rest, hence it's velocity is also zero at $t_M = 0$.

But to avoid the singularity problems in the beginning, we provide very small values to these quantities. Hence the position, velocity & attitude rates of the missile are inilized as below:

$$\vec{V} = \begin{pmatrix} u \\ v \\ w \end{pmatrix} = \begin{pmatrix} \epsilon_u \\ \epsilon_v \\ \epsilon_w \end{pmatrix} \quad \vec{r} = \begin{pmatrix} x \\ y \\ z \end{pmatrix} = \begin{pmatrix} \epsilon_x \\ \epsilon_y \\ \epsilon_z \end{pmatrix} \quad \vec{\omega} = \begin{pmatrix} p \\ q \\ r \end{pmatrix} = \begin{pmatrix} \epsilon_p \\ \epsilon_q \\ \epsilon_r \end{pmatrix}$$

where ϵ_* denotes the small value.

3.4.5.4 Formulation of differential equation

The differential equation describing the motion of the missile are derived in the fin frame. Here 15 variables of the missile are considered are state variables. Description of all the state variables are given below.

- u_f : Velocity of the missile in X-direction in fin frame
- v_f : Velocity of the missile in Y-direction in fin frame
- w_f : Velocity of the missile in Z-direction in fin frame

- p_f : Body rate about X-direction (Roll rate) in fin frame
- q_f : Body rate about Y-direction (Pitch rate) in fin frame
- r_f : Body rate about Z-direction (Yaw rate) in fin frame
- V_x : Velocity in X-direction of Launcher frame
- V_y : Velocity in Y-direction of Launcher frame
- V_z : Velocity in Z-direction of Launcher frame
- X_M : x-coordinate of missile position in Launcher frame
- Y_M : y-coordinate of missile position in Launcher frame
- Z_M : z-coordinate of missile position in Launcher frame
- ψ : Euler angle of the missile about z-axis
- θ : Euler angle of the missile about y-axis
- ϕ : Euler angle of the missile about x-axis

3.4.5.5 Velocity of the missile

The wind velocity (if any) should also be included along with missile inertial velocities because all the aero parameters of missile in general depends on the missile velocity with respect to the wind.

Hene, if $[U_{xf} \ U_{yf} \ U_{zf}]^T$ is wind velocity in the missile body frame, then missile relative velocity w.r.t wind $\vec{V}_{rw} = \begin{pmatrix} V_{rwx} \\ V_{rwy} \\ V_{rwx} \end{pmatrix} = \begin{pmatrix} u_b - U_{xf} \\ v_b - U_{yf} \\ w_b - U_{zf} \end{pmatrix}$

Where $[u_b \ v_b \ w_b]^T$ is missile inertial velocity in body frame, and can be obtained by transformation of missile velocity in fin frame as below:

$$\begin{aligned} u_b &= u_f \\ v_b &= \left(\frac{v_f - w_f}{\sqrt{2}} \right) \\ w_b &= \left(\frac{v_f + w_f}{\sqrt{2}} \right) \end{aligned}$$

Hence, the total velocity of the missile (used for aerodynamic parameter calculation) is given by

$$V_T = \sqrt{V_{rwx}^2 + V_{rwy}^2 + V_{rwx}^2}$$

3.4.5.6 Total Angle-of-Attack

The angle of attack (α_f) and angle of side slip (β_f) in fin frame in correspondence to the convention of α and β as explained in section 3.4.4, and are given by the following equations

$$\alpha_f = \tan^{-1} \left(\frac{V_{rwx} - V_{rwy}}{\sqrt{2} V_{rwz}} \right)$$

$$\beta_f = \tan^{-1} \left(\frac{V_{rwx} + V_{rwy}}{\sqrt{2} V_{rwz}} \right)$$

In the case of no wind the above expression reduces to the following equations

$$\alpha_f = \tan^{-1} \left(\frac{w_f}{u_f} \right)$$

$$\beta_f = \tan^{-1} \left(\frac{v_f}{u_f} \right)$$

The resultant angle of attack, denoted by α_R can be calculated as below

$$\alpha_R = \tan^{-1} \left(\sqrt{\tan^2 \alpha_f + \tan^2 \beta_f} \right)$$

3.4.5.7 Aerodynamic Roll orientation

The roll orientation of the missile (ϕ_a) is required for the proper resolution of aerodynamic forces and moments into reference frames (Fin Frame in this case) and quadrant in which this roll is oriented should also be calculated as follows:

$$\phi_a = \tan^{-1} \left(\frac{\beta_f}{\alpha_f} \right)$$

$$\text{I Quadrant : } \phi_a = \tan^{-1} \left(\frac{\beta_f}{\alpha_f} \right)$$

$$\text{II Quadrant : } \phi_a = \pi - \tan^{-1} \left(\frac{\beta_f}{\alpha_f} \right)$$

$$\text{III Quadrant : } \phi_a = \pi + \tan^{-1} \left(\frac{\beta_f}{\alpha_f} \right)$$

$$\text{IV Quadrant: } \phi_a = 2\pi - \tan^{-1} \left(\frac{\beta_f}{\alpha_f} \right)$$

3.4.5.8 Atmospheric Module

Input:

Altitude : X_M

The atmospheric model used for simulation is the Indian Standard Atmosphere, which assumes a homogeneous ideal dia-atmospheric gas atmosphere having a certain temperature profile with altitude (obtained by experiments).

Using this atmospheric model we compute the free stream static pressure (P_{atm}), density (ρ_{atm}) and velocity of sound (V_{sound}) at any given altitude. Which is further used in the calculation of dynamic pressure (Q) and mach no (M) of the missile.

$$\text{Dynamic Pressure, } Q = \frac{1}{2} \rho_{atm} V_T^2$$

$$\text{Mach No, } M = \frac{V_M}{V_{sound}}$$

3.4.5.9 Propulsion Module

Input:

- Time
- Atmospheric Pressure

The data is provided as thrust and mass variation with respect to time. The required thrust and mass are interpolated from this data at any given time.

Thrust:

Mangitude of instantaneous thrust (F_p) can be calculated at any given pressure by using the following formula [7]

$$F_p = F_{P_{ref}} + (P_{ref} - P_a) A_e, N$$

Where

F_P : Magnitude of instantaneous thrust, N

$F_{P_{ref}}$: Manitude of reference thrust as obtained by interpolation of test data, N

P_{ref} : Reference ambient pressure, Pa

P_a : Instantaneous ambient pressure, Pa

A_e : Nozzle exit diameter, m^2

Mass:

Mass of the missile is obtained from the input data by interpolation at required time.

3.4.5.10 Aerodynamic coefficients calculation

The Aerodynamic coefficients (C_N, C_m, C_S, C_l, C_n) are function of Mach No (M), angle-of-attack (α) and Roll angle (ϕ). This data is stored as 2-D lookup table for different roll angles (0, 22.5, 45.0, 90 deg). These values are interpolated for given mach number, angle of attack and roll angle.

The coefficients ($C_{N_\delta}, X_{CP_\delta}, C_{roll_\delta}$) are calculated by interpolation of 1D look-up table for the given mach number.

The coefficient of drag is a function of mach number and altitude which is also stored as 2D look-up table and interpolated for given mach number and altitude.

Chapter 4

Controller Design

Generally missile autopilot suffers from the problems of instability due to their highly nonlinear and uncertain aerodynamic characteristics. At large angles of attack or at high maneuvering zones, missile flight dynamics become highly nonlinear, due to significant amount of cross-coupling between the three motion axes. Also, almost all missiles have significant nonlinearities, associated with limitations in the movement of aerodynamic control surfaces. The other forms of uncertainties are namely as model variations in mass, inertia and C.G position, aerodynamic tolerances, air data sytem tolerances, structral modes and actuator failures.

4.1 Objective

The fault tolerant controller will be designed according to the following qualitative objectives

- 1) In a fault-free mode of operation, the state $x(t)$ should track the reference vector $x_d(t)$ as closely as possible, even in the possible presence of modelling uncertainty.
- 2) When a fault occurs, the controller should be able to guarantee some stability property, such as boundedness of signals in a closedloop system.
- 3) The control action $u(t)$ generated by the controller should accommodate the fault that has occured and recover the tracking performance.

4.2 Uncertain nonlinear missile dynamical model

To illustrate the effectiveness of Fault Tolerant Controller (FTC), a multi-variable nonlinear system is considered, which is a modified version of the missile 6 DOF model represented in the Eqn (3.9), as

$$\begin{aligned}\dot{u}_f &= r_f v_f - q_f w_f + \frac{1}{m} [T_x - QSC_D^0] - g_x \\ \dot{v}_f &= p_f v_f - r_f u_f + \frac{1}{m} \left[T_y + QS \left\{ C_{NB} + C_n^{\delta_y} \delta_y + \frac{d}{2V_T} \left(-C_y^{\dot{\beta}} \dot{\beta} + C_y^{r_f} r_f \right) \right\} \right] - g_y\end{aligned}$$

$$\begin{aligned}
\dot{w}_f &= q_f u_f - p_f v_f + \frac{1}{m} \left[T_z + QS \left\{ C_{NA} - C_m^{\delta_p} \delta_p + \frac{d}{2V_T} \left(-C_y^{\alpha_f} \dot{\alpha}_f + C_z^{q_f} q_f \right) \right\} \right] - g_z \\
\dot{p}_f &= \frac{1}{I_{xx}} \left[-I_{xx} p_f + M_x - (I_{zz} - I_{yy}) q_f r_f + QSd \left(C_l - C_l^{\delta_r} \delta_r + \frac{d}{2V_T} C_l^{p_f} p_f \right) \right] \\
\dot{q}_f &= \frac{1}{I_{yy}} \left[-I_{yy} q_f + M_y - (I_{xx} - I_{zz}) p_f r_f + QSd (C_{MA} - C_m^{\delta_p} \delta_p) + QSd \frac{d}{2V_T} \left(C_m^{q_f} q_f + C_m^{\alpha_f} \dot{\alpha}_f \right) \right] + \mathbf{f}_{\mathbf{Sp}} \\
\dot{r}_f &= \frac{1}{I_{zz}} \left[-I_{zz} r_f + M_z - (I_{yy} - I_{xx}) p_f q_f + QSd (C_{MB} - C_n^{\delta_y} \delta_y) + QSd \frac{d}{2V_T} \left(C_n^{r_f} r_f + C_n^{\beta_f} \dot{\beta}_f \right) \right] + \mathbf{f}_{\mathbf{Sy}}
\end{aligned} \tag{4.1}$$

Where f_{sp} and f_{sy} are *actuator fault functions* in pitch and yaw channels respectively. $f_{S*} = 0$ represents the actuator fault-free case, where as $0 < f_{S*} \leq 1.0$ represents the loss of actuator effectiveness in the pitch and yaw channels.

In simulation, the actuator faults are created as [3]

$$\begin{aligned}
f_{sp} &= \begin{cases} 0 & t < 2 \text{ sec} \\ 0.5 + 0.2 \sin(4\pi t) & 2 \leq t < 8 \text{ sec} \\ 0 & \text{else} \end{cases} \\
f_{sy} &= \begin{cases} 0 & t < 2 \text{ sec} \\ 0.5 + 0.2 \cos(4\pi t) & 2 \leq t < 8 \text{ sec} \\ 0 & \text{else} \end{cases}
\end{aligned} \tag{4.2}$$

4.3 Design of FTC

We will design a Fault Tolerant Controller for the above uncertain nonlinear system described by Eqn (4.1), by using a *Two-Time scale Redesign* technique as explained in section 2.1

On comparison of Eqn (4.1), with uncertain general multi-variable nonlinear dynamic system described by

$$\dot{x} = f(x) + g(x)(u + \delta(x)) \tag{4.3}$$

(This is the same system of Eqn 2.1 with each variable as defined there itself.)

$$f(x) = \begin{pmatrix} f_1(x) \\ f_2(x) \\ f_3(x) \\ f_4(x) \\ f_5(x) \\ f_6(x) \end{pmatrix} = \begin{pmatrix} r_f v_f - q_f w_f + \frac{1}{m} [T_x - QSC_D^0] - g_x \\ p_f v_f - r_f u_f + \frac{1}{m} \left[T_y + QS \left\{ C_{NB} + \frac{d}{2V_T} \left(-C_y^{\dot{\beta}} \dot{\beta} + C_y^{r_f} r_f \right) \right\} \right] - g_y \\ q_f u_f - p_f v_f + \frac{1}{m} \left[T_z + QS \left\{ C_{NA} + \frac{d}{2V_T} \left(-C_y^{\alpha_f} \alpha_f + C_z^{q_f} q_f \right) \right\} \right] - g_z \\ \frac{1}{I_{xx}} \left[-I_{xx} p_f + M_x - (I_{zz} - I_{yy}) q_f r_f + QSD \left(C_l + \frac{d}{2V_T} C_l^{p_f} p_f \right) \right] \\ \frac{1}{I_{yy}} \left[-I_{yy} q_f + M_y - (I_{xx} - I_{zz}) p_f r_f + QSD C_{MA} + QSD \frac{d}{2V_T} \left(C_m^{q_f} q_f + C_m^{\alpha_f} \alpha_f \right) \right] \\ \frac{1}{I_{zz}} \left[-I_{zz} r_f + M_z - (I_{yy} - I_{xx}) p_f q_f + QSD C_{MB} + QSD \frac{d}{2V_T} \left(C_n^{r_f} r_f + C_n^{\beta_f} \beta_f \right) \right] \end{pmatrix} \quad (4.4)$$

control input u is defined as $u = \begin{pmatrix} \delta_r \\ \delta_p \\ \delta_y \end{pmatrix}$,

$$g(x) = \begin{pmatrix} 0 & 0 & 0 \\ 0 & 0 & \frac{QSC_n^{\delta_y}}{m} \\ 0 & \frac{-QSC_m^{\delta_p}}{m} & 0 \\ \frac{-QSDC_l^{\delta_r}}{I_{xx}} & 0 & 0 \\ 0 & \frac{-QSDC_m^{\delta_p}}{I_{yy}} & 0 \\ 0 & 0 & \frac{-QSDC_n^{\delta_y}}{I_{zz}} \end{pmatrix} \triangleq \begin{pmatrix} 0 & 0 & 0 \\ 0 & 0 & k_{iz} D_y \\ 0 & -k_{iy} D_p & 0 \\ -D_r & 0 & 0 \\ 0 & -D_p & 0 \\ 0 & 0 & -D_y \end{pmatrix} \quad (4.5)$$

and $g(x)\delta(x) \triangleq \begin{pmatrix} \Delta f_1(x) \\ \Delta f_2(x) \\ \Delta f_3(x) \\ \Delta f_4(x) \\ \Delta f_5(x) \\ \Delta f_6(x) \end{pmatrix} + \Delta g(x) u + \begin{pmatrix} 0 \\ 0 \\ 0 \\ 0 \\ f_{Sp} \\ f_{Sy} \end{pmatrix} \quad (4.6)$

with $\|\delta(x)\| \leq \delta_i$, where δ_i is known value i.e $\delta(x)$ is norm bounded.

where $k_{iz} = \frac{I_{zz}}{md}$, $k_{iy} = \frac{I_{yy}}{md}$ & Δf_i for $i = 1$ to 6 are errors due to perturbation in aero coefficients; $\Delta g(x)$ is perturbation in $g(x)$

Let us define a variable, y as $y = h(x) = \begin{pmatrix} p_f \\ q_f \\ r_f \end{pmatrix} \quad (4.7)$

$$\text{So, } G(x) \triangleq L_g h(x) = \frac{\partial h(x)}{\partial x} g(x) = \begin{pmatrix} \frac{\partial p_f}{\partial u_f} & \frac{\partial p_f}{\partial v_f} & \frac{\partial p_f}{\partial w_f} & 1 & \frac{\partial p_f}{\partial q_f} & \frac{\partial p_f}{\partial r_f} \\ \frac{\partial q_f}{\partial u_f} & \frac{\partial q_f}{\partial v_f} & \frac{\partial q_f}{\partial w_f} & \frac{\partial q_f}{\partial p_f} & 1 & \frac{\partial q_f}{\partial r_f} \\ \frac{\partial r_f}{\partial u_f} & \frac{\partial r_f}{\partial v_f} & \frac{\partial r_f}{\partial w_f} & \frac{\partial r_f}{\partial p_f} & \frac{\partial r_f}{\partial q_f} & 1 \end{pmatrix} \begin{pmatrix} 0 & 0 & 0 \\ 0 & 0 & k_{iz} D_y \\ 0 & -k_{iy} D_p & 0 \\ -D_r & 0 & 0 \\ 0 & -D_p & 0 \\ 0 & 0 & -D_y \end{pmatrix} =$$

$$\begin{pmatrix} 0 & 0 & 0 & 1 & 0 & 0 \\ 0 & 0 & 0 & 0 & 1 & 0 \\ 0 & 0 & 0 & 0 & 0 & 1 \end{pmatrix} \begin{pmatrix} 0 & 0 & 0 \\ 0 & 0 & k_{ix}D_y \\ 0 & -k_{iy}D_p & 0 \\ -D_r & 0 & 0 \\ 0 & -D_p & 0 \\ 0 & 0 & -D_y \end{pmatrix} = \begin{pmatrix} -D_r & 0 & 0 \\ 0 & -D_p & 0 \\ 0 & 0 & -D_y \end{pmatrix} \quad (4.8)$$

To estimate the unknown $\delta(x)$ we will design the filter, as represented by Eqn. (2.5)

$$\begin{aligned} \dot{\hat{y}} &= L_f h(x) + G(x)u - \frac{1}{\epsilon} (\hat{y} - y), \quad \hat{y}(0) = y(0) \\ \Rightarrow \begin{pmatrix} \dot{\hat{p}}_f \\ \dot{\hat{q}}_f \\ \dot{\hat{r}}_f \end{pmatrix} &= \begin{pmatrix} f_4(x) - D_r \delta_r \\ f_5(x) - D_p \delta_p \\ f_6(x) - D_y \delta_y \end{pmatrix} - \frac{1}{\epsilon} \begin{pmatrix} \hat{p}_f - p_f \\ \hat{q}_f - q_f \\ \hat{r}_f - r_f \end{pmatrix} \end{aligned} \quad (4.9)$$

$$\text{Define a variable } l, \text{ as per Eqn (2.6), } l \triangleq \begin{pmatrix} \frac{\hat{p}_f - p_f}{\epsilon} \\ \frac{\hat{q}_f - q_f}{\epsilon} \\ \frac{\hat{r}_f - r_f}{\epsilon} \end{pmatrix} \quad (4.10)$$

Therefore a desired controller, u_{des} to cancel the effect of $\delta(x)$ in Eqn (4.1) is

$$u_{des}(\mathbf{x}) = u_{nom}(\mathbf{x}) + G^{-1}(\mathbf{x}) \mathbf{l}(\mathbf{x}) \quad (4.11)$$

Where $u_{nom}(x)$ is the *Nominal control law* for the nominal system represened by Eqn (3.9)

4.3.1 Design of Nominal Controller $u_{nom}(x)$

To design nominal controller $u_{nom}(x)$ in Eqn (4.11), a Two-Time Scale Separation technique is adopted for the nominal system described by Eqn (3.9). Since the slow and fast subsystems consists of three first order differential equations each, with relative degree (1,1,1). So the resulting control law makes six degrees of freedom appear, corresponding to the six first order time constant of each channel, for both the slow and fast subsystems. Tuning these constants as a matter of fact, it can be done through considerations similar to those employed in the classical linear autopilot design approach [2].

The actuator dynamics must be really faster than the fast subsystem. It turns out that, by using small gain theorem, this condition can be expressed in terms of frequency magnitude conditions, involving the transfer function of the neglected higher dynamics and the transfer function of the ideal closed loop system.

The *Two-Time Scale Separation* design technique as explained in detail in section 2.2 of Chapter-2, is applied to the nominal system described by Eqn (3.9). In this approach, states p_f , q_f and r_f are identified as faster dynamic responses, while α_f , β_f and ϕ_f are characterized as slow state variables. The angular rates p_f , q_f and r_f strongly depends upon the fin deflection. Thus to start with fast state controller, states p_f , q_f and r_f are designed. Having designed a fast state controller, a separate approximate inversion procedure was carried out, to design the slow state controller for α_f , β_f and ϕ_f . It may be noted that, such a model reduction was possible as there was significant difference in time scale between the fast and slow states in the open loop dynamics of the missile.

As stated earlier, the design of this controller depends on two time scale separation. The *outer loop* has slow dynamics and the *inner loop* has faster dynamics. The outer loop controller takes the commanded acceleration and current acceleration as input and generates the rate command which works as a input to the inner loop. The basic block diagram of the Time scale separated nonlinear controller is shown in the Fig 4.1

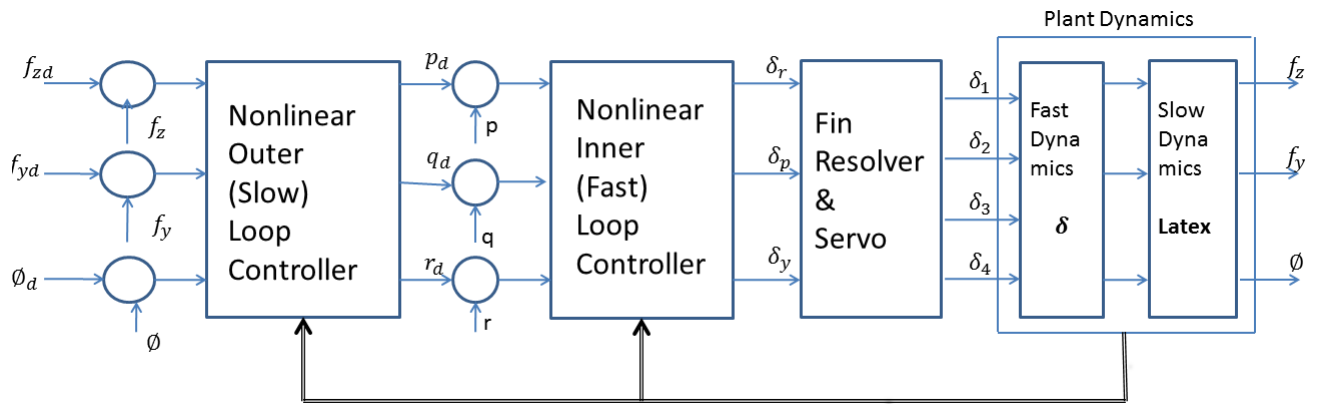


Fig 4.1: Two-Time Scale Separation Autopilot Configuration

4.3.1.1 Inner-Loop Design formulation with NDI technique

The control structure of the inner loop is similar as outer loop structure. The purpose of this inner-loop design is to decouple the Roll, Pitch and Yaw channels and the equivalent transfer function between the control input v_I and output y_I (suffix I stands for Inner-loop) for states p_f , q_f and r_f taken independently, is that of an integrator.

Here, in our problem there are three inputs and three outputs are available.

The fast subsystem dynamics are stated as $\dot{x}_f = f_f(x) + G_f(x) u$; with output $y_f = h_f(x_f, u)$.

Here fast states $x_f = (p_f \ q_f \ r_f)^T$ and full state vector $x = (u_f \ v_f \ w_f \ p_f \ q_f \ r_f)^T$ is of dimension 6x1 . output vector $y_f = (p_f \ q_f \ r_f)^T$ is 3x1 vector . $f(x)$ and $h(x)$ are smooth vector fields and $G_f(x)$ is 6x3 matrix, whose columns are also smooth vector fields.

Recalling the governing equations as presented in chapter-3 (Eqn 3.9) the output equation is

$$\begin{aligned} \dot{p}_f &= \frac{1}{I_{xx}} \left[-I_{xx} p_f + M_x - (I_{zz} - I_{yy}) q_f r_f + Q S d \left(C_l - C_l^{\delta_r} \delta_r + \frac{d}{2V_T} C_l^{p_f} p_f \right) \right] \\ \dot{q}_f &= \frac{1}{I_{yy}} \left[-I_{yy} q_f + M_y - (I_{xx} - I_{zz}) p_f r_f + Q S d \left(C_{MA} - C_m^{\delta_p} \delta_p \right) + Q S d \frac{d}{2V_T} \left(C_m^{q_f} q_f + C_m^{\dot{\alpha}_f} \dot{\alpha}_f \right) \right] \\ \dot{r}_f &= \frac{1}{I_{zz}} \left[-I_{zz} r_f + M_z - (I_{yy} - I_{xx}) p_f q_f + Q S d \left(C_{MB} - C_n^{\delta_y} \delta_y \right) + Q S d \frac{d}{2V_T} \left(C_n^{r_f} r_f + C_n^{\dot{\beta}_f} \dot{\beta}_f \right) \right] \end{aligned} \quad (4.12)$$

The system relative degree is $r_1 = 1, r_2 = 1, r_3 = 1$. The above equation may be written as

$$\begin{aligned} \begin{pmatrix} y_1^{(r_1)} \\ y_2^{(r_2)} \\ y_3^{(r_3)} \end{pmatrix} &= \begin{pmatrix} L_f^{r_1} h_1(x) \\ L_f^{r_2} h_2(x) \\ L_f^{r_3} h_3(x) \end{pmatrix} + E_I(x) \begin{pmatrix} \delta_r \\ \delta_p \\ \delta_y \end{pmatrix} \\ \Rightarrow \begin{pmatrix} \dot{p}_f \\ \dot{q}_f \\ \dot{r}_f \end{pmatrix} &= M_I(x) + E_I(x) \begin{pmatrix} \delta_r \\ \delta_p \\ \delta_y \end{pmatrix} ; \text{ Where} \end{aligned} \quad (4.13)$$

$$M_I(x) = \begin{pmatrix} L_f h_1(x) \\ L_f h_2(x) \\ L_f h_3(x) \end{pmatrix} = \begin{pmatrix} \frac{1}{I_{xx}} \left[-I_{xx} p_f + M_x - (I_{zz} - I_{yy}) q_f r_f + Q S d \left(C_l + \frac{d}{2V_T} C_l^{p_f} p_f \right) \right] \\ \frac{1}{I_{yy}} \left[-I_{yy} q_f + M_y - (I_{xx} - I_{zz}) p_f r_f + Q S d C_{MA} + Q S d \frac{d}{2V_T} \left(C_m^{q_f} q_f + C_m^{\dot{q}_f} \dot{q}_f \right) \right] \\ \frac{1}{I_{zz}} \left[-I_{zz} r_f + M_z - (I_{yy} - I_{xx}) p_f q_f + Q S d C_{MB} + Q S d \frac{d}{2V_T} \left(C_n^{r_f} r_f + C_n^{\dot{r}_f} \dot{r}_f \right) \right] \end{pmatrix} \quad (4.14)$$

and the decoupling matrix,

$$E_I(x) = \begin{pmatrix} L_{g_1} h_1(x) & L_{g_2} h_1(x) & L_{g_3} h_1(x) \\ L_{g_1} h_2(x) & L_{g_2} h_2(x) & L_{g_3} h_2(x) \\ L_{g_1} h_3(x) & L_{g_2} h_3(x) & L_{g_3} h_3(x) \end{pmatrix} = \begin{pmatrix} \frac{-Q S d C_l^{\delta_r}}{I_{xx}} & 0 & 0 \\ 0 & \frac{-Q S d C_m^{\delta_p}}{I_{yy}} & 0 \\ 0 & 0 & \frac{-Q S d C_n^{\delta_y}}{I_{zz}} \end{pmatrix} = \begin{pmatrix} -D_r & 0 & 0 \\ 0 & -D_p & 0 \\ 0 & 0 & -D_y \end{pmatrix} \quad (4.15)$$

The 3x3 matrix $E_I(x)$ is invertible over the region. Then the input transformation

$$u = \begin{pmatrix} \delta_r \\ \delta_p \\ \delta_y \end{pmatrix} = E_I^{-1}(x) \begin{pmatrix} v_{I1} - L_f^{r1} h_1(x) \\ v_{I2} - L_f^{r2} h_2(x) \\ v_{I3} - L_f^{r3} h_3(x) \end{pmatrix} \quad (4.16)$$

(or)

$$u = \begin{pmatrix} \delta_r \\ \delta_p \\ \delta_y \end{pmatrix} = -E_I^{-1}(x) M_I(x) + E_I^{-1}(x) \begin{pmatrix} v_{I1} \\ v_{I2} \\ v_{I3} \end{pmatrix} \quad (4.17)$$

Where the vector $v_I = (v_{I1} \ v_{I2} \ v_{I3})^T$ is the new control input obtained by designing the linear controller so that the relationship between the plant output and the new control input v_I is linear and decoupled.

The above three equations of the simple form $\begin{pmatrix} \dot{p}_f \\ \dot{q}_f \\ \dot{r}_f \end{pmatrix} = \begin{pmatrix} v_{I1} \\ v_{I2} \\ v_{I3} \end{pmatrix}$. Hence the control law decouples the longitudinal and lateral motion. Here reference inputs $(v_{I1} \ v_{I2} \ v_{I3})$ are calculated as follow

$$\begin{pmatrix} v_{I1} \\ v_{I2} \\ v_{I3} \end{pmatrix} = \begin{pmatrix} \dot{p}_f \\ \dot{q}_f \\ \dot{r}_f \end{pmatrix} = \begin{pmatrix} \frac{\delta_{rBS}}{\tau_{qf}} \\ \frac{q_{fref} - q_f}{\tau_{rf}} \\ \frac{r_{fref} - r_f}{\tau_{rf}} \end{pmatrix} = \begin{pmatrix} \delta_{rBS} \\ (q_{fref} - q_f) \omega_{qf} \\ (r_{fref} - r_f) \omega_{rf} \end{pmatrix}$$

To robustify the roll performance, against unwanted roll disturbances, roll autopilot is carried out by integrator backstepping as we will see in forth coming sections of this chapter. This means that, new control input v_{I1} is equated to roll control law $\delta_{r_{BS}}$ as obtained from backstepping roll autopilot design.

4.3.1.2 Outer-loop design formulation using NDI

The command to the outer loop is the demanded lateral acceleration generated by the guidance law as per missile target kinematics. The outer loop basically controls the flight path rate of the missile. The outer loop generates the body rate demand to the inner loop. Therefore, the plant considered for outer loop in which, input is body rate and output is lateral acceleration. The control structure of the outer loop is shown in the Fig 4.2

Referring the governing equation, the output may be expressed, as represented by Eqn (3.11)

$$\begin{aligned}\dot{\phi}_f &= p_f - (q_f \sin\phi_f + r_f \cos\phi_f) \cot\alpha_R + \frac{(a_y \cos\phi_f - a_z \sin\phi_f)}{V_T \sin\alpha_R} \\ \dot{\alpha}_f &= q_f - (p_f \cos\alpha_f + r_f \sin\alpha_f) \cos\alpha_f \tan\beta_f + \frac{(a_z \cos\alpha_f - a_x \sin\alpha_f) \cos\alpha_f}{\frac{V}{\sqrt{1+\tan^2\alpha+\tan^2\beta}}} \alpha_f \\ \dot{\beta}_f &= -r_f + (p_f \cos\beta_f + q_f \sin\beta_f) \cos\beta_f \tan\alpha_f + \frac{(a_y \cos\beta_f - a_x \sin\beta_f) \cos\beta_f}{\frac{V}{\sqrt{1+\tan^2\alpha+\tan^2\beta}}}\end{aligned} \quad (4.18)$$

The above equation may be written in companion form as

$$\begin{pmatrix} \dot{\phi}_f \\ \dot{\alpha}_f \\ \dot{\beta}_f \end{pmatrix} = f_s(x) + g_s(x) \begin{pmatrix} p_f \\ q_f \\ r_f \end{pmatrix} \quad (4.19)$$

$$\text{Where, } f_s(x) = \begin{pmatrix} \frac{(a_y \cos\phi_f - a_z \sin\phi_f)}{V_T \sin\alpha_R} \\ \frac{(a_z \cos\alpha_f - a_x \sin\alpha_f) \cos\alpha_f}{\frac{V}{\sqrt{1+\tan^2\alpha+\tan^2\beta}}} \\ \frac{(a_y \cos\beta_f - a_x \sin\beta_f) \cos\beta_f}{\frac{V}{\sqrt{1+\tan^2\alpha+\tan^2\beta}}} \end{pmatrix} \triangleq \begin{pmatrix} f_\phi(x) \\ f_\alpha(x) \\ f_\beta(x) \end{pmatrix};$$

$$g_s(x) = \begin{pmatrix} 1 & -\sin\phi_f \cot\alpha_R & -\cos\phi_f \cot\alpha_R \\ -\cos^2\alpha_f \tan\beta_f & 1 & \sin\alpha_f \cos\alpha_f \tan\beta_f \\ \cos^2\beta_f \tan\alpha_f & \sin\beta_f \cos\beta_f \tan\alpha_f & -1 \end{pmatrix} \triangleq \begin{pmatrix} 1 & g_{1q} & g_{1r} \\ g_{2p} & 1 & g_{2r} \\ g_{3p} & g_{3q} & -1 \end{pmatrix}$$

Hence the Eqn (4.19) may be rewritten as

$$\begin{pmatrix} \dot{\phi}_f \\ \dot{\alpha}_f \\ \dot{\beta}_f \end{pmatrix} = \begin{pmatrix} f_\phi(x) \\ f_\alpha(x) \\ f_\beta(x) \end{pmatrix} + \begin{pmatrix} 1 & g_{1q} & g_{1r} \\ g_{2p} & 1 & g_{2r} \\ g_{3p} & g_{3q} & -1 \end{pmatrix} \begin{pmatrix} p_f \\ q_f \\ r_f \end{pmatrix} \quad (4.20)$$

Since, α_f and β_f are not measurable quantities, so they are derived from the measurable quantities f_z and f_y (Latex demand) by using the following relation.

$$f_z = \frac{\rho V_T^2 S C_{N\alpha}}{2m} \left(1 - \frac{h}{l_c}\right) \quad (4.21)$$

$$f_y = \frac{\rho V_T^2 S C_{N\beta}}{2m} \left(1 - \frac{h}{l_c}\right)$$

Where ρ is the air density, V_T is the missile velocity, S is the reference area, m is mass of the missile, h is the *static margin* and l_c is the control moment arm.

Differentiating Eqn (4.21), we get

$$\dot{f}_z = \frac{\partial f_z}{\partial \alpha_f} \dot{\alpha}_f \quad (4.22)$$

$$\dot{f}_y = \frac{\partial f_y}{\partial \beta_f} \dot{\beta}_f$$

$$\text{Where } \frac{\partial f_z}{\partial \alpha_f} = \frac{\rho V_T^2 S C_{N\alpha}}{2m} \left(1 - \frac{h}{l_c}\right) \text{ and } \frac{\partial f_y}{\partial \beta_f} = \frac{\rho V_T^2 S C_{N\beta}}{2m} \left(1 - \frac{h}{l_c}\right)$$

from Equation 4.22, we can write $\dot{\alpha}_f = \left(\frac{\partial f_z}{\partial \alpha_f}\right)^{-1} \dot{f}_z$; $\dot{\beta}_f = \left(\frac{\partial f_y}{\partial \beta_f}\right)^{-1} \dot{f}_y$

$$\text{Where } \dot{f}_z = \frac{(a_{zf \text{ ref}} - a_{zf})}{\tau_{zf}} = (a_{zf \text{ ref}} - a_{zf}) \omega_{zf} \text{ and } \dot{f}_y = \frac{(a_{yf \text{ ref}} - a_{yf})}{\tau_{yf}} = (a_{yf \text{ ref}} - a_{yf}) \omega_{yf}$$

Now applying feedback linearization law for Eqn (4.20)

$$\begin{pmatrix} p_f \\ q_f \\ r_f \end{pmatrix} = \begin{pmatrix} 1 & g_{1q} & g_{1r} \\ g_{2p} & 1 & g_{2r} \\ g_{3p} & g_{3q} & -1 \end{pmatrix}^{-1} \left\{ \begin{pmatrix} \dot{\phi}_f \\ \dot{\alpha}_f \\ \dot{\beta}_f \end{pmatrix} - \begin{pmatrix} f_\phi(x) \\ f_\alpha(x) \\ f_\beta(x) \end{pmatrix} \right\} \quad (4.23)$$

The above equation linearizes the slow dynamics. If the desired linearized command is $(\phi_{fd} \ \alpha_{fd} \ \beta_{fd})^T$, applying the body rate input to the Equation 4.23 transforms into the following form

$$\begin{pmatrix} \dot{\phi}_{fd} \\ \dot{\alpha}_{fd} \\ \dot{\beta}_{fd} \end{pmatrix} = \begin{pmatrix} \dot{\phi}_f \\ \dot{\alpha}_f \\ \dot{\beta}_f \end{pmatrix} = \begin{pmatrix} v_{O1} \\ v_{O2} \\ v_{O3} \end{pmatrix}; \text{ Where suffix } O \text{ stands for output.}$$

From the above two loop designs, we can conclude that, the obtained body rates $(p_f \ q_f \ r_f)$ from the outer loop, is given to inner loop to get the roll, pitch and yaw fin deflections $(\delta_r \ \delta_p \ \delta_y)$ as we can call it as nominal controller $u_{nom}(x)$. Hence the nominal controller can be written from Equation 4.16 as shown in Eqn (4.33)

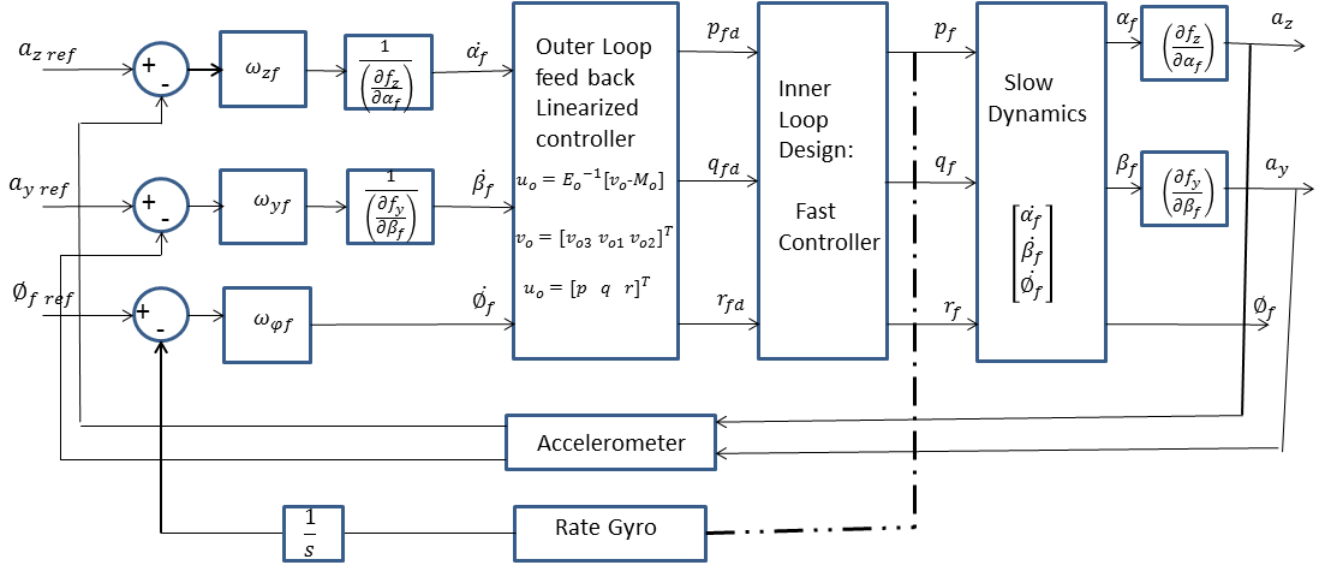


Fig 4.2 : Control structure of Nonlinear Outer loop design

4.3.1.3 Roll Autopilot Design Via Integrator Backstepping

Unlike aircraft, there is no strongly stable position in roll for cruciform, cartesian controlled missiles, and therefore they tend to roll due to various undesirable rolling moments such as the ones arising from airframe misalignments, asymmetrical loading of the lift and control surfaces, fin biases, and atmospheric disturbances. In most missiles the roll position is required to be stabilized because the unwanted rolling motion leads several undesired effects.

For missiles that are stabilized in roll position, the pitch and yaw channels can be considered as decoupled single-input and single-output systems, thereby greatly

simplifying the design of the autopilots.

So, in this work we employed an *integrator backstepping technique* for the design of the roll autopilot, as with this technique system nonlinearities do not have to be cancelled in control law. If a nonlinearity acts stabilizing, and thus in a sense is useful, it may be retained in the closed loop system. This leads to robustness to model errors and control effort may be needed to control the system.

Let us formulate the roll autopilot design problem [2].

We have to track a desired roll angle ϕ^* . By letting $\phi^* = 0$ it degenerates to regular problem.

Let $\sigma \triangleq \phi - \phi^*$, then $\dot{\sigma} = \dot{\phi} - \dot{\phi}^* = p$.

So the roll channel dynamics for tracking a desired roll angle may be formulated as below

$$\begin{aligned}\dot{\sigma} &= p \\ \dot{p} &= u_{pse} = f_p + g_p \delta_r \quad (u_{pse} \text{ is pseudo control})\end{aligned}\tag{4.24}$$

Now, for the above roll dynamics, we will design pseudo control law u_{pse} , by using Integrator Backstepping control technique, as explained in section 2.2 .

For design of $\phi(x) = \phi(\sigma)$, let (refering Eqn.2.8)

$$V_1(x) = V_1(\sigma) = \frac{1}{2}\sigma^2; \dot{V}_1(\sigma) = \sigma\dot{\sigma} = \sigma p \leq -V_a(\sigma)\tag{4.25}$$

Let

$$V_a(\sigma) = k_1\sigma^2 + k_2\sigma^4 \quad (k_1, k_2 \geq 0)\tag{4.26}$$

Then from Eqns.(4.25-4.26)

$$p = \dot{\phi}(\sigma) = -k_1\sigma - k_2\sigma^3 \quad (\text{Note : when } \sigma \rightarrow 0, \phi(\sigma) \rightarrow 0)\tag{4.27}$$

Now the modified system (refer Eqn. 2.9) is

$$\dot{\sigma} = p + \phi(\sigma) - \phi(\sigma) = \phi(\sigma) + z \quad (z \triangleq p - \dot{\phi}(\sigma))\tag{4.28}$$

$$\dot{z} = v \quad (\text{where } v = \dot{p} - \dot{\dot{\phi}}(\sigma) = u_{pse} - \ddot{\phi}(\sigma))$$

Let the candidate Lyapunov function (Eqn. 2.13) be

$$V(\sigma, p) = V_1(z) + \frac{1}{2}z^2\tag{4.29}$$

Then following Eqn (2.14)

$$\dot{V}(\sigma, p) = \dot{V}_1(\sigma) + z\dot{z} = \left(\frac{\partial V_1}{\partial \sigma}\right) \dot{\sigma} + z v = \left(\frac{\partial V_1}{\partial \sigma}\right) [\phi(\sigma) + z] + z v \quad (4.30)$$

Let us select (refer Eqn 4.25)

$$v = -\left(\frac{\partial V_1}{\partial \sigma}\right) \dot{\sigma} - k_3 z - k_4 z^3 = -\sigma - k_3 z - k_4 z^3 \quad (k_3, k_4 > 0) \quad (4.31)$$

So using Eqn (4.27), Eqns (4.30-4.31)

$$\dot{V}(\sigma, p) = -k_1 \sigma^2 - k_2 \sigma^4 - k_3 z^2 - k_4 z^4 < 0 \quad (k_1, k_2, k_3, k_4 > 0; \quad \forall \sigma, p \in R^2) \quad (4.32)$$

Control selection algorithm for roll dynamics

1. Define $z = p + k_1 \sigma + k_2 \sigma^3$ ($k_1, k_2 > 0$)
2. compute $v = -\sigma - k_3 z - k_4 z^3$ ($k_3, k_4 > 0$)
3. compute $\dot{\phi}(\sigma) = (-k_1 - 3k_2 \sigma^2) p$
4. compute $u_{pse} = \dot{\phi}(\sigma) + v = (-k_1 - 3k_2 \sigma^2) p - (\sigma + k_3 z + k_4 z^3)$
5. compute $\delta_{rBS} = \frac{(u_{pse} - f_p)}{g_p}$

From the above three designs Viz. Lateral Autopilot design using Time Scale Separation technique and Roll Autopilot design using Integrator Backstepping technique, we can combine the control laws and write nominal control law as,

$$u_{nom}(x) = \begin{bmatrix} \frac{-u_{pse} + L_f h_1(x)}{D_r} \\ \frac{-v_{I2} + L_f h_2(x)}{D_p} \\ \frac{-v_{I3} + L_f h_3(x)}{D_y} \end{bmatrix} \quad (4.33)$$

4.3.2 Design of Desired controller $u_{des}(x)$

Plugging Equation (4.33), into the Equation (4.11) to get the desired control law $u_{des}(x)$, to cancel out the effect of unknown $\delta(x)$

$$u_{des}(x) = \begin{bmatrix} \frac{-u_{pse} + L_f h_1(x)}{D_r} \\ \frac{-v_{I2} + L_f h_2(x)}{D_p} \\ \frac{-v_{I3} + L_f h_3(x)}{D_y} \end{bmatrix} + \begin{pmatrix} -D_r & 0 & 0 \\ 0 & -D_p & 0 \\ 0 & 0 & -D_y \end{pmatrix}^{-1} \begin{bmatrix} \frac{\hat{p}_f - p}{\epsilon} \\ \frac{\hat{q}_f - q}{\epsilon} \\ \frac{\hat{r}_f - r}{\epsilon} \end{bmatrix} \quad (4.34)$$

Here ϵ is simulation parameter generally very small value and here we selected as $\epsilon = 0.01$ (Refer Appendix A for selecting value of ϵ)

4.4 Input data for FTC

Generally gain scheduling is carried out based on suitable aerodynamic parameter which reflect flight condition in terms of mach nuber (M), Altitude and Angle-of-Attack (α), So the parameter Turning rate time constant ($T_\alpha = \frac{m V_T}{Q S C_N^\alpha}$) is the best choice. The pitch and yaw channel gain scheduling (body rate limiters of ± 60 deg/sec) is as follow

Autopilot time constant is given by $\tau_{ap} = 0.10 T_\alpha$

So, $\omega_0 \left(\omega_{fy} = \omega_{fz} = \frac{1}{\tau_{fy}} = \frac{1}{\tau_{fz}} \right) = \min \left\{ 8.0, \frac{1}{\tau_{ap}} \right\}$ for outer loop of two-time separation design (To calculate \dot{f}_z and \dot{f}_y latex commands)

$\omega_{in} \left(\omega_{qf} = \omega_{rf} = \frac{1}{\tau_{qf}} = \frac{1}{\tau_{rf}} \right) = \min \{ 25.0, 2.5 \omega_0 \}$ for inner loop of two-time scale separation design (To calculate \dot{q}_f and \dot{r}_f commands)

The uncertainty on aerodynamic data along with fault funtion over Nominal Controller, for present Fault Tolerant Controller design is taken as

$$\begin{aligned} \Delta C_D^0 &= \pm 10\% C_D^0 & \Delta C_L &= \pm 10\% C_L & \Delta C_m &= \pm 10\% d C_L \\ \Delta C_y &= \pm 10\% C_y & \Delta C_m^q &= \pm 10\% d C_y & \Delta C_l^0 &= \pm 20\% C_l^0 \\ \Delta C_L^\delta &= \pm 15\% C_L^\delta & \Delta C_m^\delta &= \pm 15\% d C_L^\delta & \Delta C_l^{\delta r} &= \pm 15\% C_l^{\delta r} \end{aligned}$$

Case study #1

The test profile of controller as autopilot demand along Roll, Pitch, Yaw as a function of time is given below. Here along roll channel $\phi_d = 0$ throughout. Lateral acceleration demand along pitch channel is -20g along (8-10) seconds and 10g along (12-17) seconds and for yaw is 20g along (5-7) seconds and 10g along (12-17) seconds.

Parameter	Autopilot demand at different time zones												
Time (sec)	0.4	5.0	5.1	7.0	7.001	8.0	8.1	10.0	10.001	12.0	12.01	17.0	17.01
Roll demand(ϕ_d)	0.0	0.0	0.0	0.0	0.0	0.0	0.0	0.0	0.0	0.0	0.0	0.0	0.0
Pitch demand(f_z)	0.0	0.0	0.0	0.0	0.0	0.0	-20g	-20g	0.0	0.0	10g	10g	0.0
Yaw demand(f_y)	0.0	0.0	20g	20g	0.0	0.0	0.0	0.0	0.0	0.0	10g	10g	0.0

Table 4.1: Autopilot demand at different time zones for case study-1

Case study #2

The test profile of controller as autopilot demand along Roll, Pitch, Yaw as a function of time is given below. Here roll channel demand is 10g along (5-7) seconds and -10g along (8-10) seconds. Lateral acceleration demand for pitch is 10g along (5-7) seconds and -15g along (8-10) seconds and for yaw is 20g along (5-7) seconds and -15g along (8-10) seconds.

Parameter	Autopilot demand at different time zones												
Time (sec)	0.4	5.0	5.1	7.0	7.001	8.0	8.1	10.0	10.001	12.0	12.01	17.0	17.01
Roll demand(ϕ_d)	0.0	0.0	10g	10g	0.0	0.0	-10g	-10g	0.0	0.0	0.0	0.0	0.0
Pitch demand(f_z)	0.0	0.0	10g	10g	0.0	0.0	-15g	-15g	0.0	0.0	0.0	0.0	0.0
Yaw demand(f_y)	0.0	0.0	20g	20g	0.0	0.0	-15g	-15g	0.0	0.0	0.0	0.0	0.0

Table 4.2: Autopilot demand at different time zones for case study-2

The above designed controller performace is compared in the above given two test cases i.e case #1 and case #2 with respect to nominal controller that is with out actuator fault and uncertainties.

Chapter 5

Performance of Controller

5.1 Simulation Platform and Input data

A *MATLAB* Code is programmed to simulate the full scale 6-DOF of the missile dynamics. A Nominal TwoTime Scale Separation technique based, nonlinear Lateral Autopilot (Pitch and Yaw) and Integrator Backstepping technique based Roll Autopilot is also cosdired along with Fault Tolerant Controller for performance comparison.

All the wind tunnel aerodynamic parameters are used here as a look up table. A second order actuation servo system is included into the control loop. All the physical limitations of the actuation system i.e Dead Zone, Command Saturation and Rate Saturation are cosidered.

The differential equations are numerically solved using **Runga Kutta 4** method.

The missile being surface to air application, initially it will coming out of launcher at around 400 m/s from $T_0(u, v, w) = (45.0, 5.0, 5.0)$ m/s and the body rates $(p, q, r) = (27.0, 13.0, 2.0)$ deg/s and $(\psi, \theta, \phi) = (0.0, 55.0, 0.0)$ deg has been considered. Initially the body pitch, yaw rate has been controlled ($q_{fd} = r_{fd} = 0$) upto 2 seconds of flight time and later (a_{yf}, a_{zf}) demand has been tracked upto 10 seconds. In roll channel, $\phi_d = 0$ for skid-to-turn flight vehicle.

Missile mass $m = (155-100)$ Kg, x_{cg} from nose = $(2.0-1.7)$ m, $I_{xx} = (0.95-0.76)$ $kg-m^2$, $I_{yy} = (156-126)$ $kg-m^2$, $I_{zz} = (161-131)$ $kg-m^2$ at $(0.0-7.0)$ seconds. During 7 seconds of powered flight, thrust=1800 kgf

5.2 Simulation Results

5.2.1 Performance comparison for Case study #1

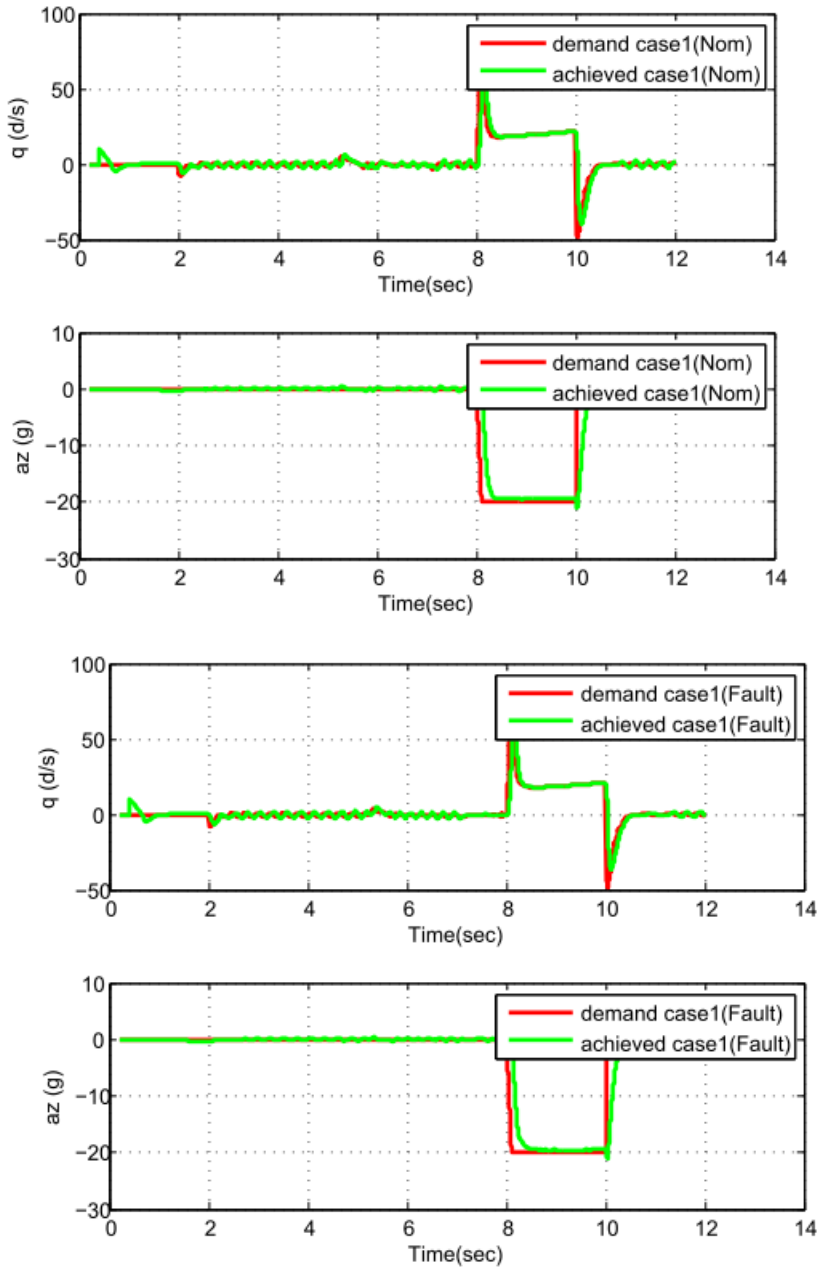


fig 5.1: Comparative tracking performance of Latex Pitch command and pitch rate(Case 1)

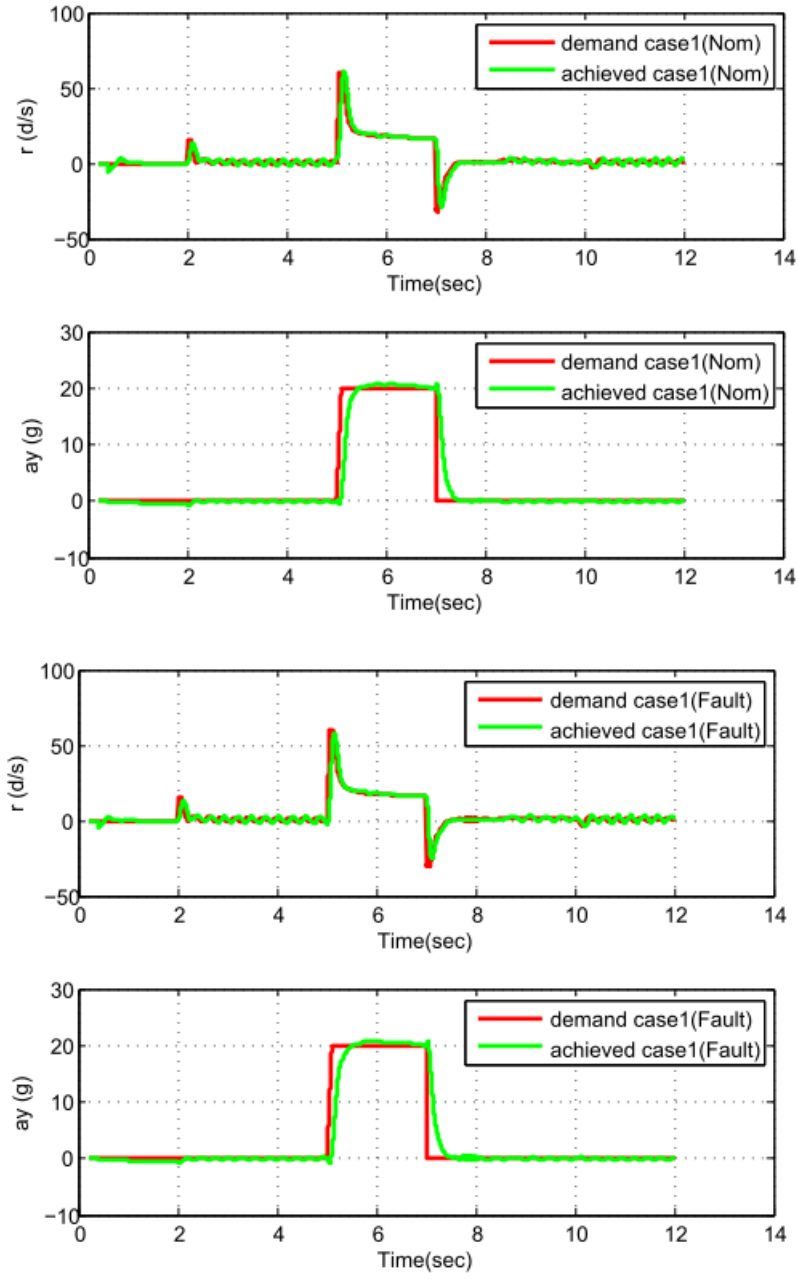


fig 5.2: Comparative tracking performance of Latex Yaw command and Yaw rate (Case 1)

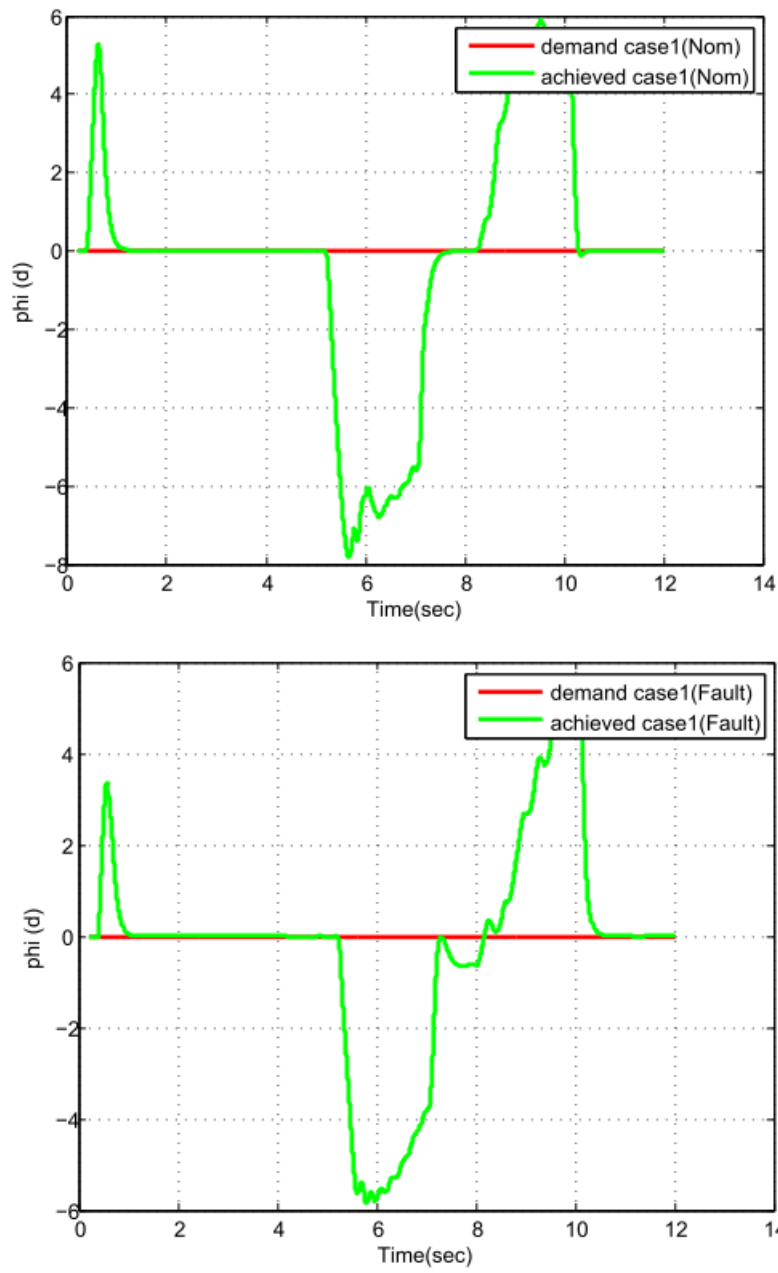


fig 5.3 : Comparative tracking performance of Roll demand (Case-1)

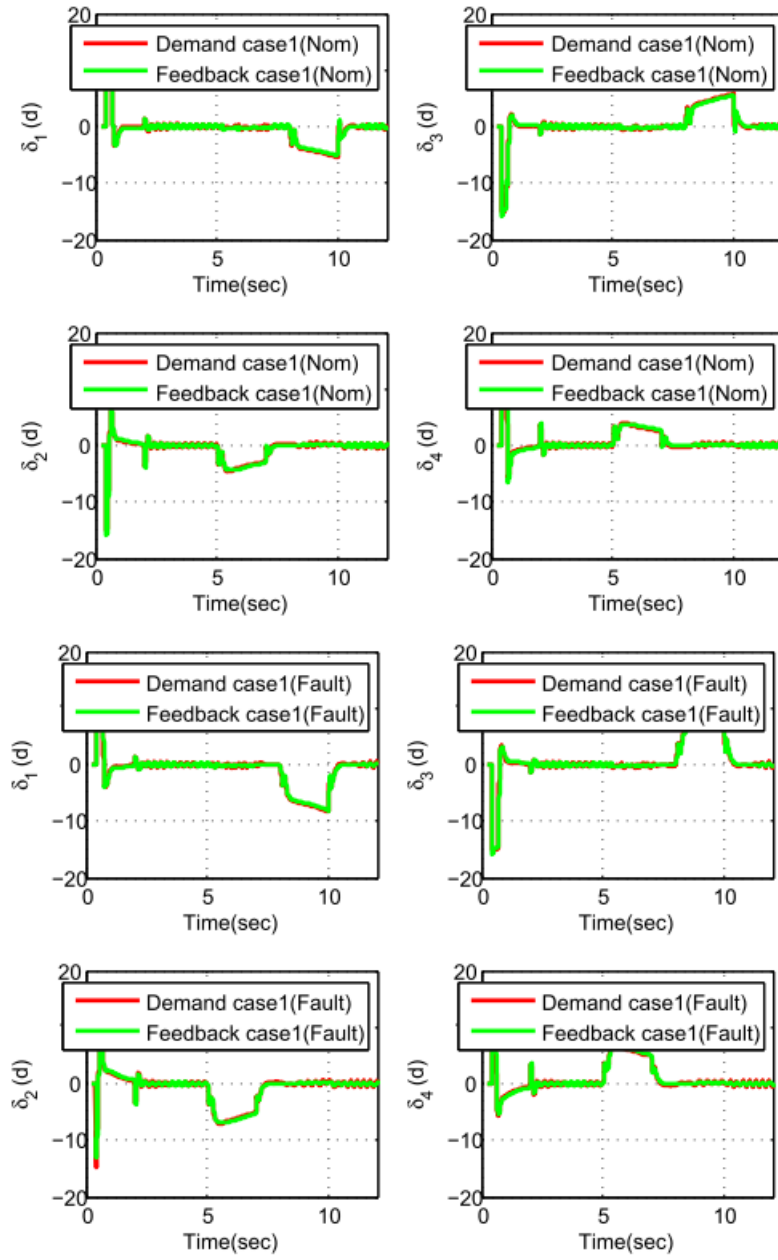


fig 5.4 : Comparative fin deflection time profiles (Case-1)

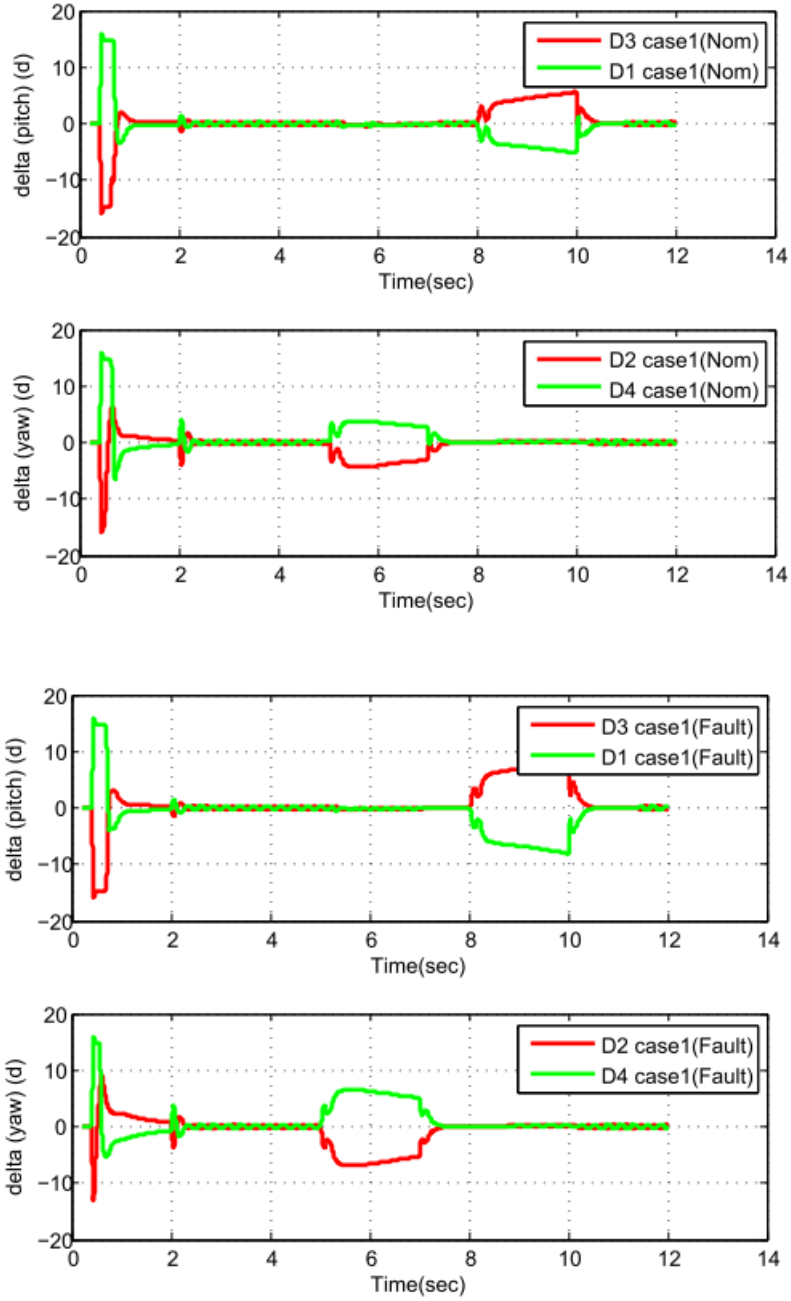


fig 5.5 : Comparative performance of Pitch & Yaw deflection (δ_p δ_y) time profiles (Case-1)

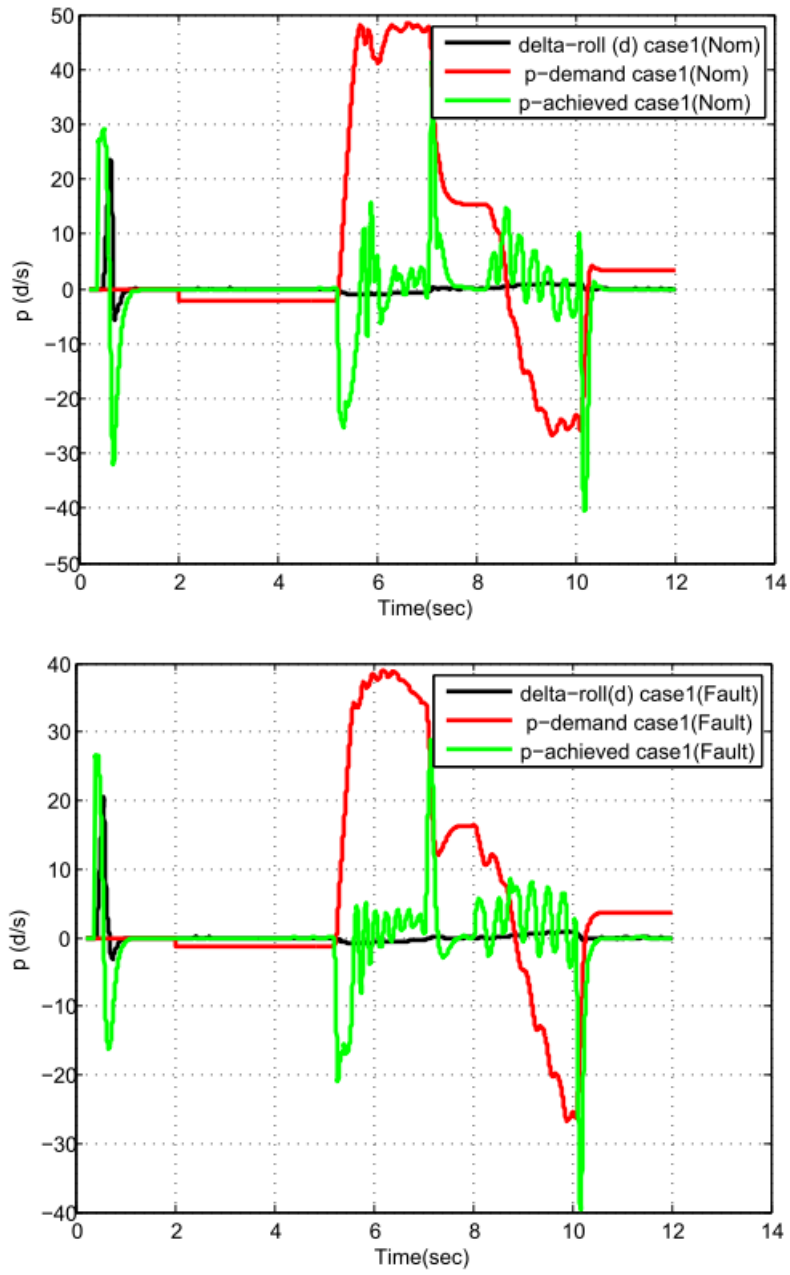


fig 5.6 : Comparative tracking performance of Roll rate (p_f) and Roll deflection (δ_r) for Case-1

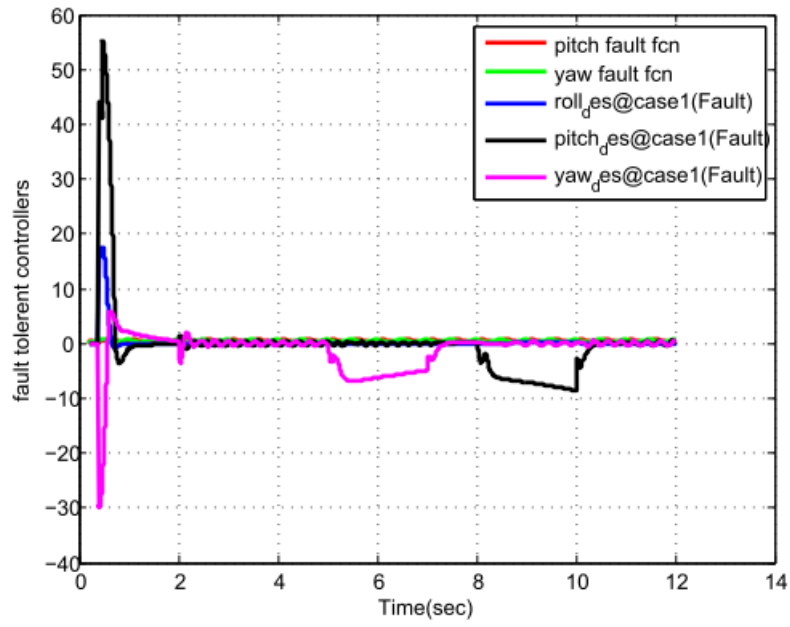
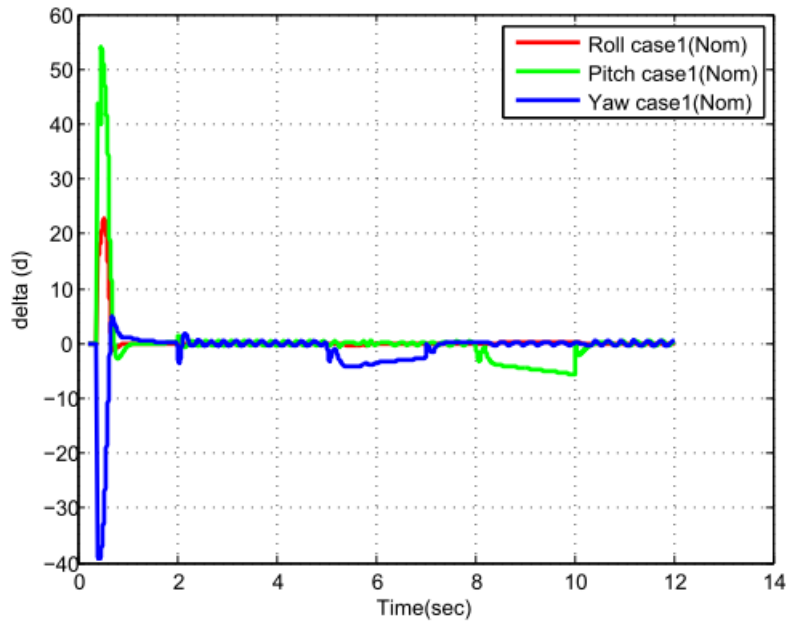


fig 5.7 : Comparative control law (δ_r , δ_p , δ_y) time profiles (Case-1)

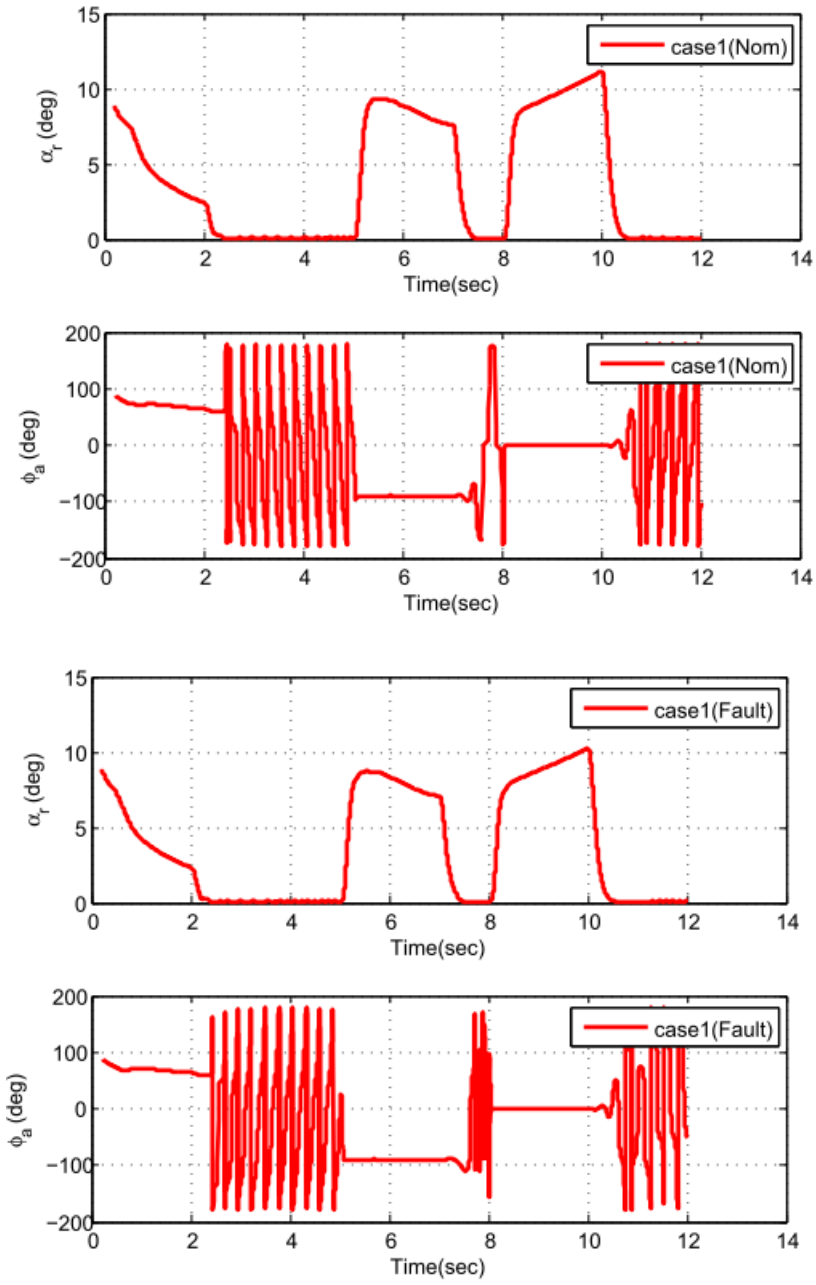


fig 5.8 : Comparative performance of Angle-of-Attack & Roll Orientation time profiles (Case-1)

5.2.2 Performance comparison of Case study #2

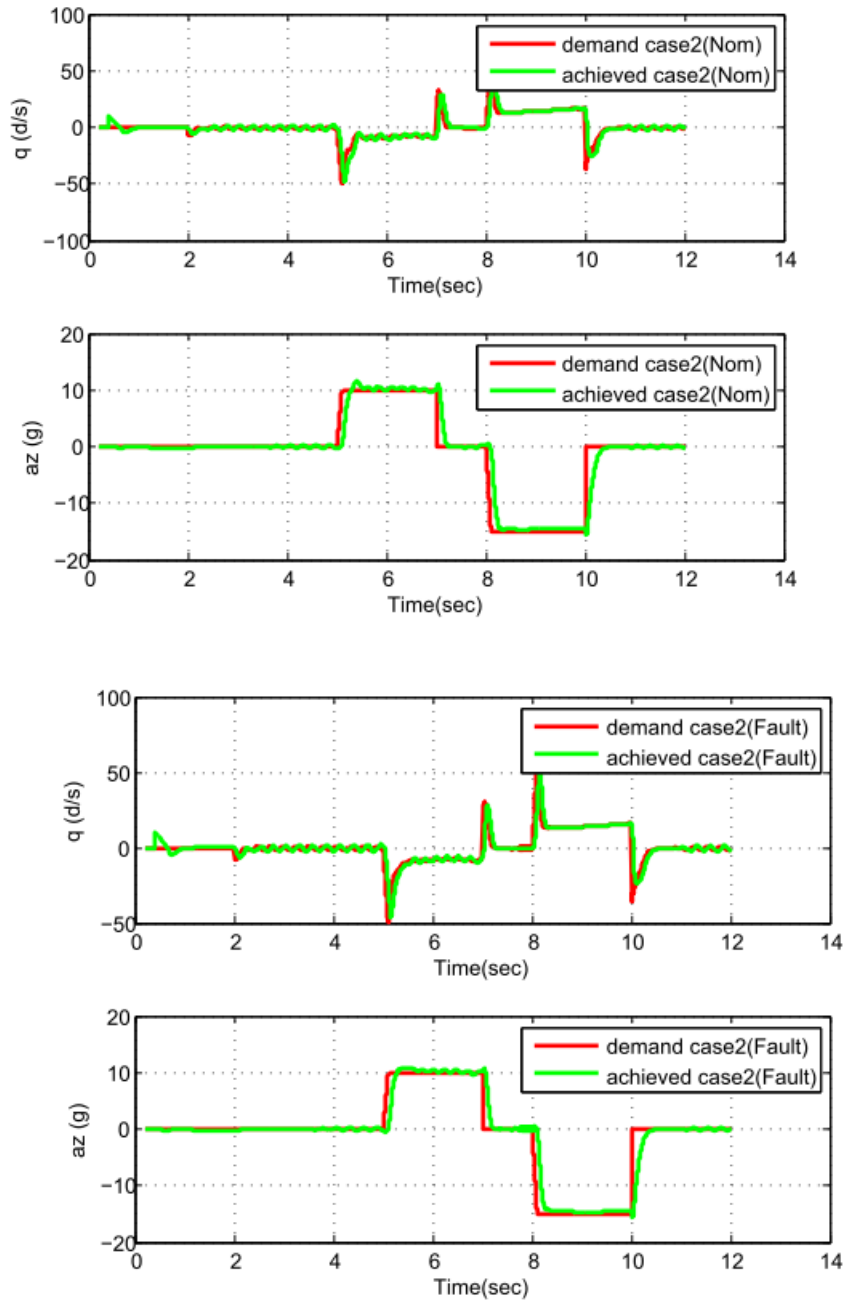


fig 5.9 : Comparative tracking performance of Latex Pitch command and pitch rate(Case-2)

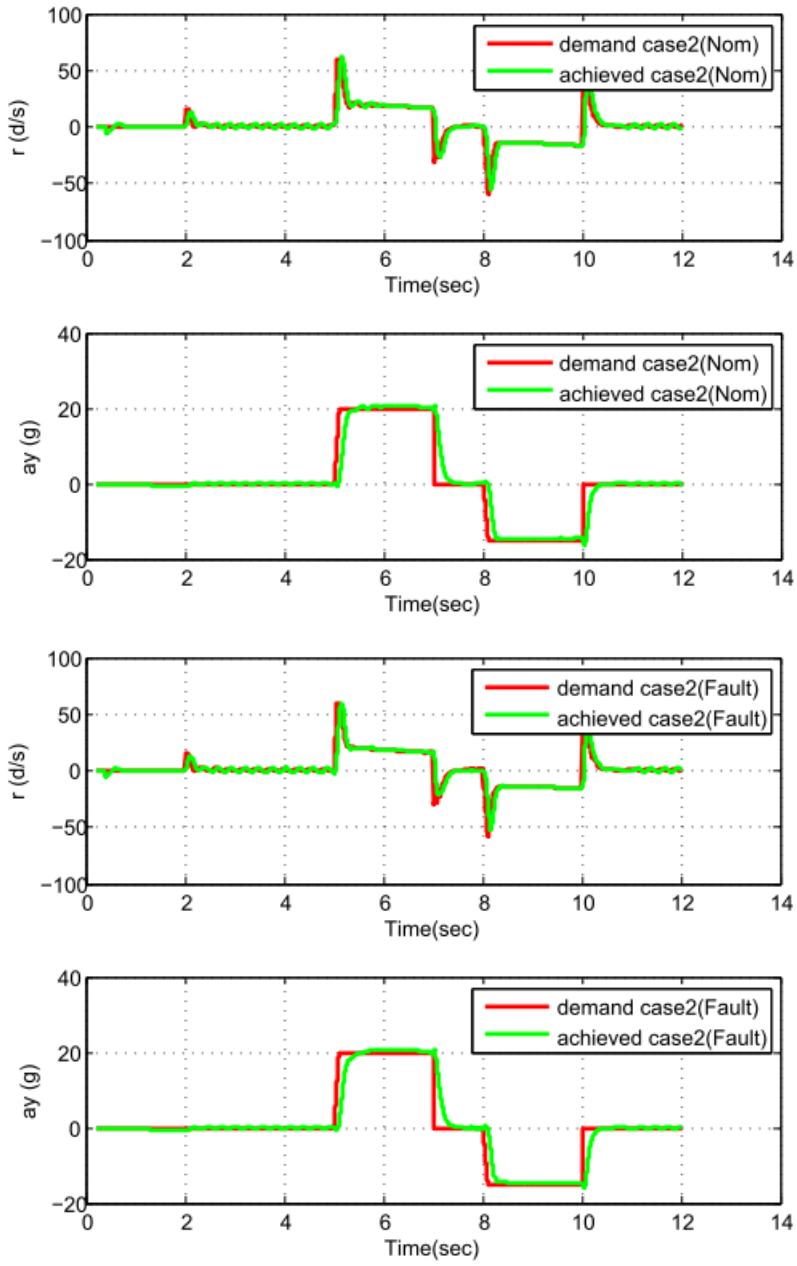


fig 5.10 : Comparative tracking performance of Latex Yaw command and Yaw rate (Case-2)

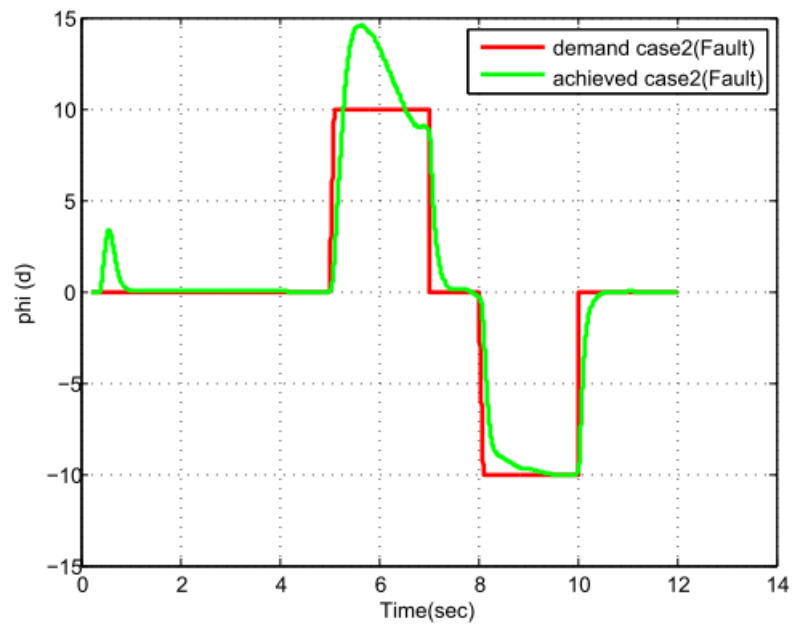
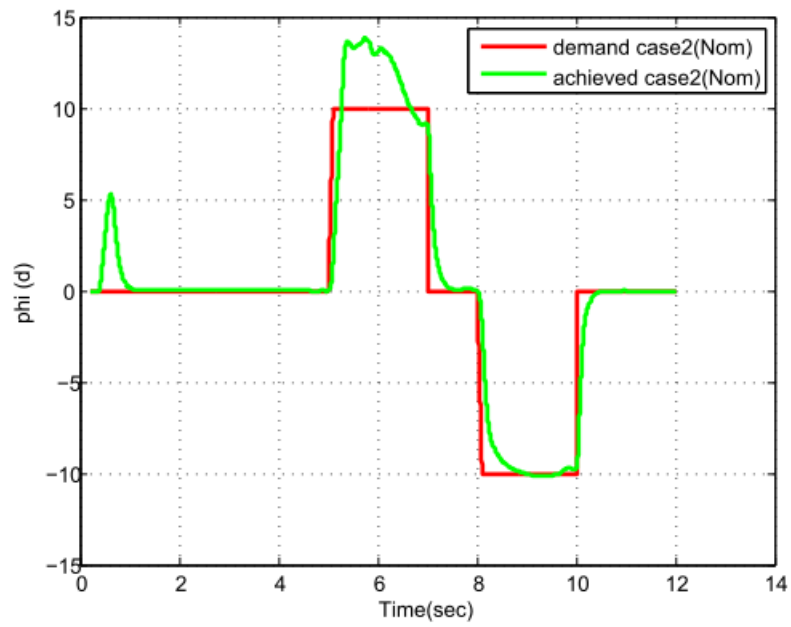


fig 5.11 : Comparative tracking performance of Roll demand (Case-2)

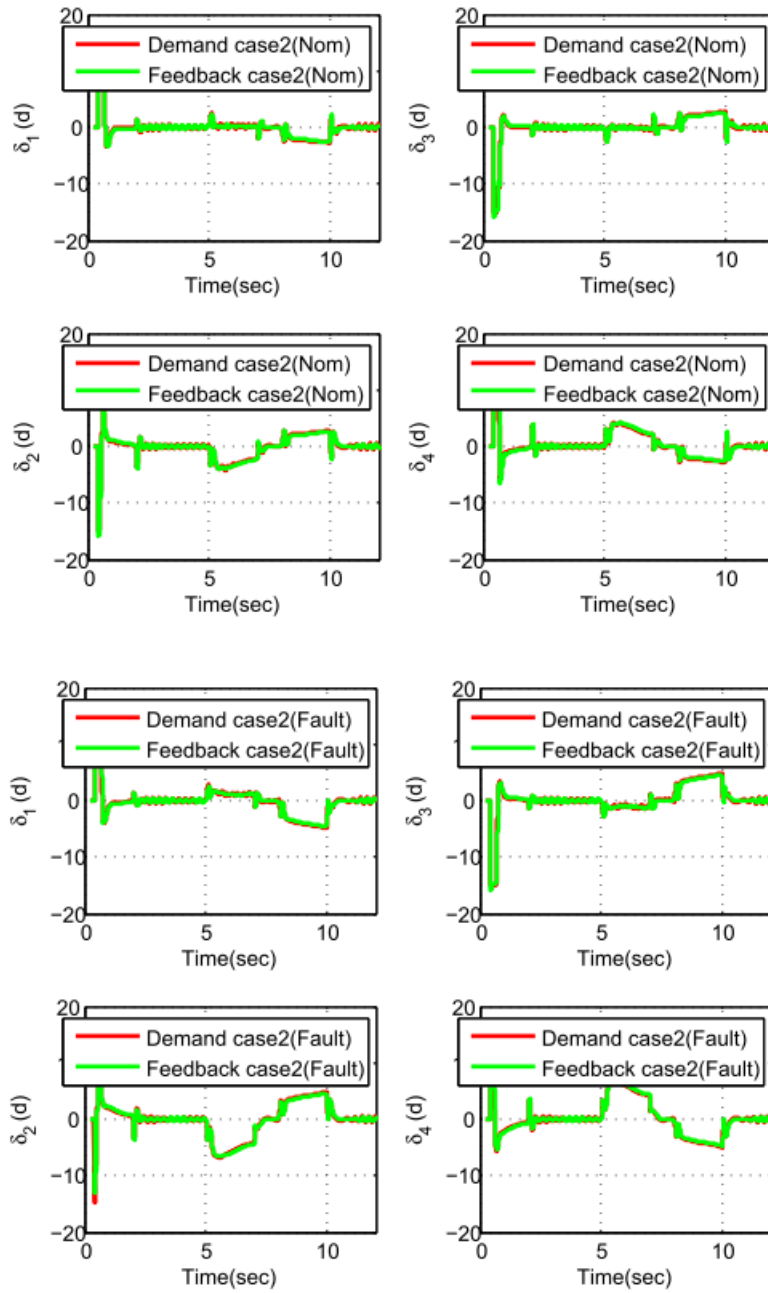


fig 5.12 : Comparative fin deflection time profiles (Case-2)

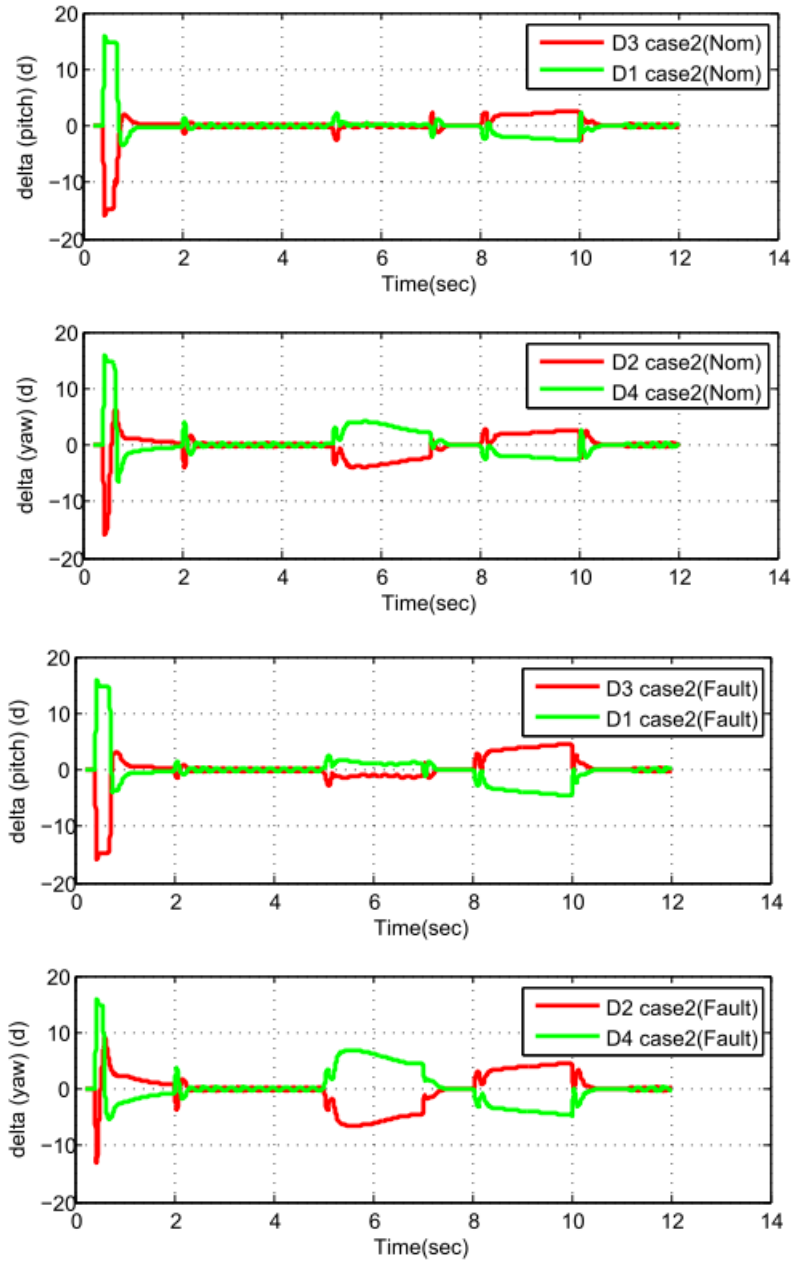


fig 5.13: Comparative performance of Pitch & Yaw deflection (δ_p δ_y) time profiles (Case-2)

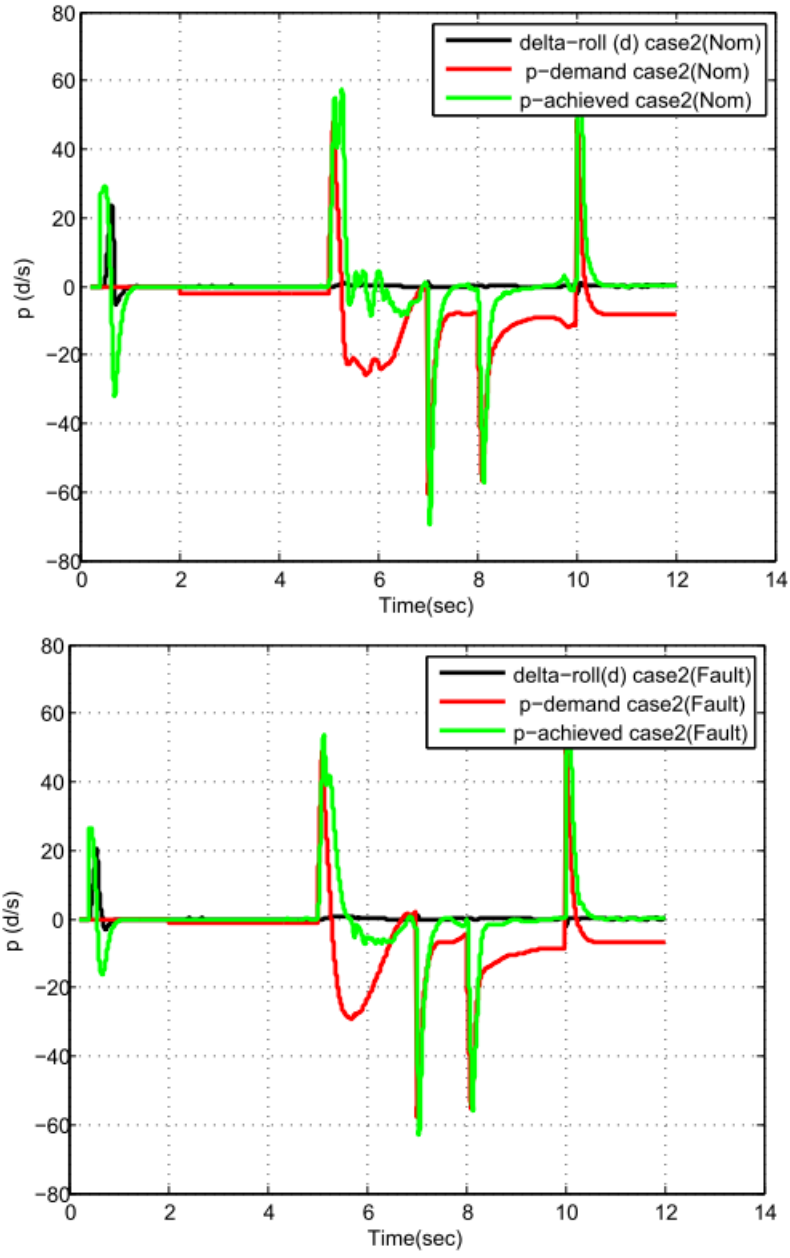


fig 5.14 : Comparative trackig performance of Roll rate (p_f) and Roll deflection (δ_r)for Case-2

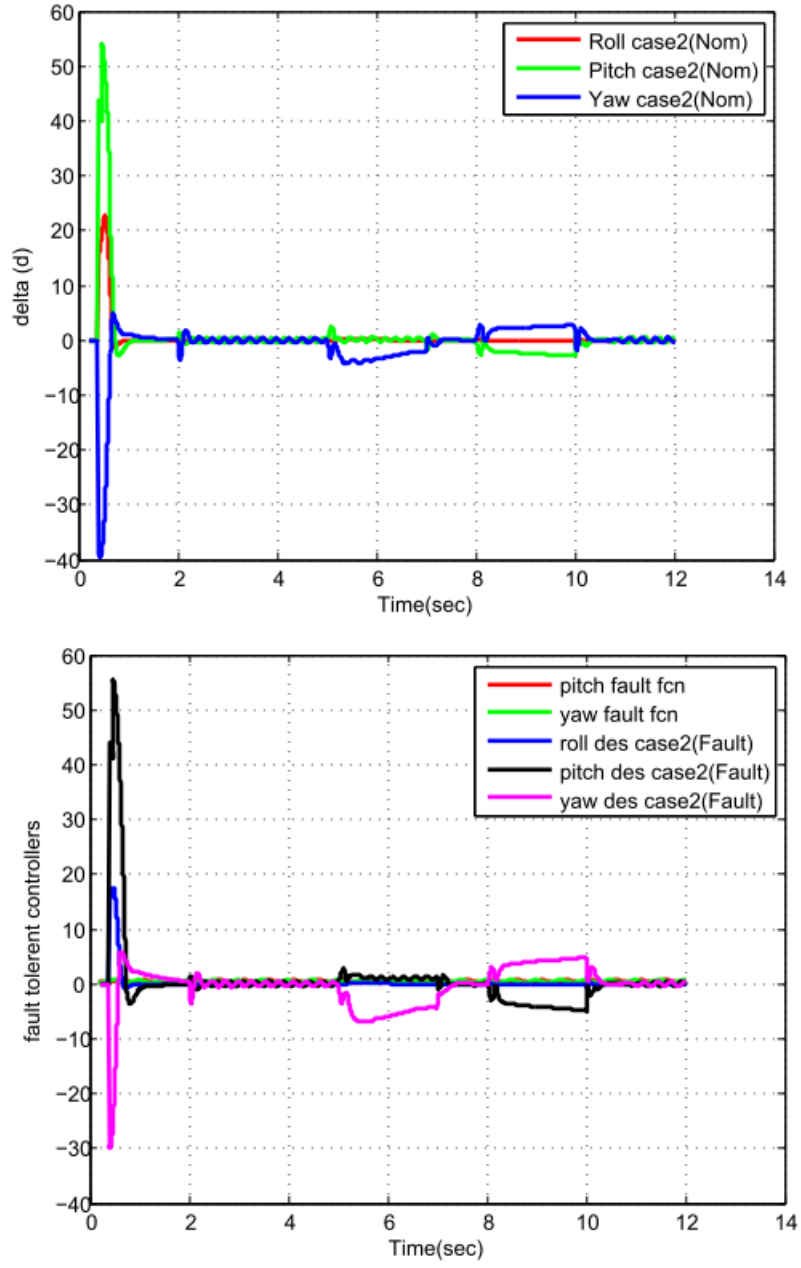


fig 5.15 : Comparative control law (δ_r , δ_p , δ_y) time profiles (Case-2)

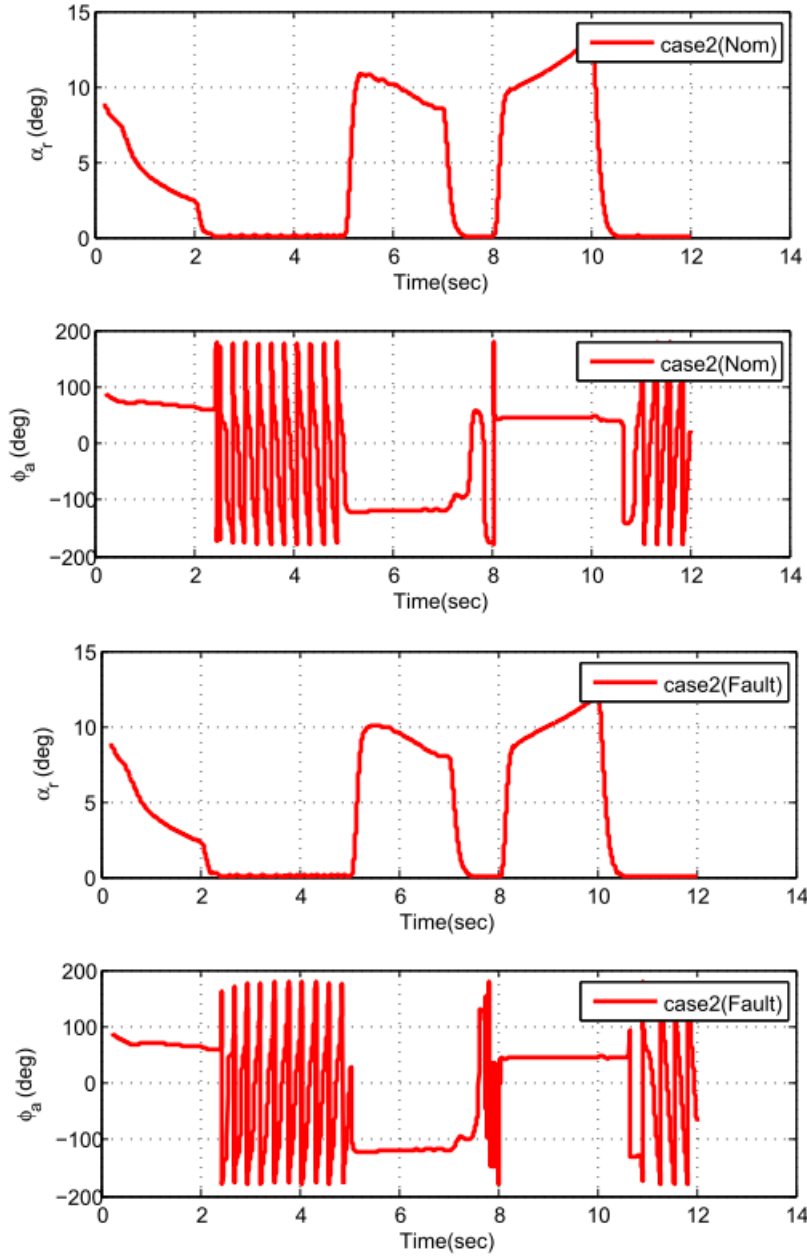


fig 5.16 : Comparative performance of Angle-of-Attack & Roll Orientation time profiles (Case-2)

Chapter-6

Conclusion & Future Directions

6.1 Conclusions

This research demonstrates the design of Fault Tolerant Controller (FTC) in the area of missile control problem associated with actuator faults and high plant uncertainty. This FTC design methodology is carried out in *Two-Time scale redesign* technique with basic principle is that, the fast variables arising from designed high-gain filter in the nominal feedback control law in order to cancel the effect of uncertainties in the plant, so that after a fast transient the closed loop trajectories converge to the nominal trajectories.

Being a two stage design of FTC Viz. Nominal controller design and High-gain filter design, *Time Scale Separation* and *Integrator Backstepping* techniques are applied to design the former. The design of FTC is validated here through a full scale 6-DOF simulation considering detailed parameter uncertainties and sinusoidal nature of actuator faults. A comparison is also made with nominal controller (plant without faults and uncertainties) to bring out the salient features of the FTC design considering 2 case studies.

The following variables are compared with same simulation platform

- Tracking performance of Lateral Pitch and Yaw accelerations.
- Tracking performance of Longitudinal Roll angle.
- Tracking performance of Pitch, Yaw and Roll rates.
- Tracking performance of individual fin deflections.
- Time profile of both the control laws.
- Time history of Angle-of-Attack and Roll orientation.

Comparing the 6-DOF simulation results, the following salient features of the FTC design may be noted

- There is no significant change in the transient response of the states of uncertain system, in two case studies.
- It does not alter the nature of decoupling among the roll, pitch and yaw motion axis.
- It does not alter the nature of fast time response of both latas as well as body rates. This feature indicates the quick correction and as a result it improves mission terminal performance such as miss distance and impact angle, even the actuators are malfunctioning.

All these features imply on improvement of terminal performance of the interceptor even against actuator faults and plant uncertainties. Hence, this research work may give a significant contribution in the field of guidance and control of missile.

6.2 Future Directions

The design is validated through 6-DOF simulation, where the measurements are considered noise free. Only measurement error of constant bias value is considered for simulation and performance analysis. The design should be validated through *Monte Carlo* simulation considering realistic measurement noise spectrum. This task can be carried out in future.

Flight control and guidance loops of interceptor missiles are usually assumed to be spectrally separated. Thus a hierarchical design approach is commonly used, where an innerloop autopilot is constructed to follow the acceleration commands issued by the outer loop guidance algorithm. The guidance law is designed based on low order approximation of the autopilot dynamics. However since most guidance laws are inversely proportional to time to go, spectral separation may not be valid near interception, causing instability and, consequently unacceptable miss distances. The strong requirement of future interceptors is the hit to kill miss distance.

The integrated flight control and guidance law design may enhance the endgame performance of the interceptor by accounting the coupling between the control and

guidance dynamics. The integrated design may provide synergism between the two control components, may also postpone the endgame instability. In such a design problem, the entire guidance and control loop may be stated as a solution to the finite horizon control problem, instead of the common approach treating the inner autopilot loop and outer guidance loop separately. A considerable research effort may be required to find the potential for improved performance of an integrated autopilot guidance design. So the design of integrated autopilot guidance controller will be taken into account in future, which may minimize the miss distance and control energy under worst case target maneuvers and measurement uncertainty

Appendix A

Stability Analysis of Uncertain Nonlinear System

Theorem :- Given a compact set $\Omega_x \subset R^n$ of initial conditions there exists an $\epsilon^* > 0$ such that for all $0 < \epsilon < \epsilon^*$ and for all $x(0) \in \Omega_x$ the controller (2.5), (2.6), (2.9) guarantees boundedness of $x(t)$ to the origin.

In addition, given any $\xi > 0$, there exists an $\epsilon^{**} > 0$ such that for all $x(0) \in \Omega_x$, the solution $\bar{x}(t)$ of the nominal system (2.2) and $x(t, \epsilon)$ of the uncertain system (2.1) with the redesigned controller (2.5), (2.6), (2.9) satisfy

$$\|x(t, \epsilon) - \bar{x}(t)\| \leq \xi \quad \forall t > 0 \quad [1] \quad (A1).$$

Proof :- With the off-manifold variable

$$\eta \triangleq l + G(x) \delta(x) \quad (A2)$$

Substituting Eqn (A2) in Eqn (2.1), we get

$$\begin{aligned} \dot{x} &= f(x) + g(x) [\alpha(x) + G^{-1}l + \delta(x)] \\ &= f(x) + g(x) [\alpha(x) + G^{-1}(\eta - G\delta) + \delta] \\ &= \tilde{f}(x) + g(x) G^{-1}(x) \eta \quad \text{where } \tilde{f}(x) = f(x) + g(x) \alpha(x) \end{aligned} \quad (A3)$$

Similarly, on substitution of Eqn (A2) in Eqn (2.7), we will get

$$\epsilon \dot{\eta} = -\eta + \epsilon J(x) \left[\tilde{f}(x) + g(x) G^{-1}(x) \eta \right] \quad \text{where } J(x) = \frac{\partial(G(x)\delta(x))}{\partial x} \quad (A4)$$

For the reduced system, $\dot{x} = \tilde{f}(x)$ we need Lyapunov function satisfying (A5) below. The following Lemma shows that its existence follows from Assumption 1.

Lemma 1:- Assumption 1 implies that there exists a positive definite radially unbounded C^2 Lyapunov function $\tilde{V}(x)$ satisfying

$$\frac{\partial \tilde{V}^T}{\partial x} [f(x) + g(x) \alpha(x)] \leq -\|x\|^2 \quad \forall x \quad (A5)$$

Considering the Lyapunov function candidate as

$$W(x, \eta) = \tilde{V}(x) + \frac{\eta\eta^T}{2} \quad (A 6)$$

we have,

$$\dot{W} = \frac{\partial \tilde{V}^T}{\partial x} \left[\tilde{f}(x) + g(x) G^{-1}(x) \eta \right] - \frac{\eta\eta^T}{\epsilon} + \eta^T J(x) \left[\tilde{f}(x) + g(x) G^{-1}(x) \eta \right] \quad (A 7)$$

Because $l(0) = 0$ in (2.7), we get $\eta(0) = G(x(0))\delta(0)$ which means that for every compact set Ω_x of initial conditions $x(0)$, we can find a corresponding compact set Ω_η of initial conditions $\eta(0)$, we can find a level set Ω_c of W such that

$$\Omega_x x \Omega_\eta \subseteq \Omega_c \quad (A 8)$$

and positive numbers L_1, L_2, L_3 and L_4 such that on this level set Ω_c

$$\left\| \frac{\partial \tilde{V}}{\partial x} \right\| \leq L_1 \|x\| \quad (A 9)$$

$$\|J(x)\| \leq L_2 \quad (A 10)$$

$$\|\tilde{f}(x)\| \leq L_3 \|x\| \quad (A 11)$$

$$\|g(x) G^{-1}(x)\| \leq L_4 \quad (A 12)$$

hold. Using these inequalities, we can obtain from (A 7) and (A 8)

$$\dot{W} \leq -\|x\|^2 + L\|x\|\|\eta\| - \frac{\|\eta\|^2}{\epsilon} + L_2 L_4 \|\eta\|^2$$

where $L = L_1 L_4 + L_2 L_3$. Then, from the inequality

$$L\|x\|\|\eta\| \leq \frac{1}{2}\|x\|^2 + \frac{L^2}{2}\|\eta\|^2$$

we get

$$\dot{W} = -\frac{1}{2}\|x\|^2 - \left[\frac{1}{\epsilon} - \frac{L^2}{2} - L_2 L_4 \right] \|\eta\|^2$$

which means that for all $0 < \epsilon < \epsilon^*$ where

$$\epsilon^* = \frac{1}{L_2 L_4 + \frac{L^2}{2}} \quad (A 13)$$

Appendix B

Stability Analysis of NDI controller using Time Scale Separation

In this chapter, we are trying to analyze the closed loop stability of a nonlinear system using a two-time scale dynamic inversion controller. A state space formulation is derived, assuming the inner-loop inversion is performed exactly. A Lyapunov analysis is then performed to show that, under certain assumptions, the exponential stability of the system about constant commanded state values is guaranteed with sufficiently large inner-loop gain.

Time-scale separation exists in many dynamical systems. This phenomena can arise due to small time constants, moments of inertia, flexible body dynamics and many other effects. Using the natural separation between the *fast* and *slow* variables to reduce the complexity of a dynamical system can greatly simplify the control design and analysis problem.

Problem formulation

Let us consider a nonlinear affine control system [11]

$$\dot{x} = f(x) + g(x)y \tag{B 1}$$

$$\dot{y} = h(x,y) + k(x,y)u \tag{B 2}$$

Where $x \in R^n$ is slow states, $y \in R^n$ is fast states and $u \in R^n$ is control input.

Further suppose the following assumptions are hold

Assumption 1:- The functions $g(x)$ and $k(x,y)$ are invertible.

Assumption 2:- The functions $f(x)$, $g(x)$, $h(x,y)$ and $k(x,y)$ are finite inside a level set of a Lyapunov function V for the system, which will be defined shortly.

Assumption 3:- The derivative of $f(x)$ and $g(x)$ with respect to x are finite inside the level set of V .

Assumption 4:- The desired value of x , $x = x_c$ is constant.

The two-time scale dynamic inversion controller for the system (B1-B2) is of th

form

$$u = k^{-1}(x, y) \{ \dot{y}_d - h(x, y) \} \quad (B 3)$$

$$y_c = g^{-1}(x) \{ \dot{x}_d - f(x) \} \quad (B 4)$$

With,

$$\dot{x}_d = \Omega(x_c - x) \quad (B 5)$$

$$\dot{y}_d = \omega_i I(y_c - y) \quad (B 6)$$

and

$$\Omega = \text{Diag}(\omega_{o1}, \omega_{o2}, \dots, \omega_{on})$$

Theorem :- Suppose Assumptions (1-4) hold for the dynamical system given by equations (B1-B2) . Then, with the dynamic inversion controller specified by equations (B3-B6), the states x will be exponentially stable about their commanded values for any gain $\omega_i \geq \omega_i^*$ sufficiently large.

Proof:- The first step of the proof is to convert the dynamical system into a state-space system for x and \dot{x} only. The stability of this system will then be studied using Lyapunov analysis.

Rewrite $g(x)$ as

$$g(x) = [g_1(x), g_2(x), \dots, g_n(x)] \quad (B 7)$$

where $g_i(x)$ is $n \times 1$ vector function. Then taking the derivative of (B 1) with respect to time gives

$$\ddot{x} = \frac{\partial f}{\partial x} \dot{x} + \left[\frac{\partial g_1}{\partial x} \dot{x}, \frac{\partial g_2}{\partial x} \dot{x}, \dots, \frac{\partial g_n}{\partial x} \dot{x} \right] y + g(x) \dot{y} \quad (B 8)$$

Substituting,

$y_c = g^{-1}(x) \{ \dot{x}_d - f(x) \}$, $y = g^{-1}(x) \{ \dot{x} - f(x) \}$ and $\dot{y} = \omega_i I(y_c - y)$ into equation (B 8) gives

$$\ddot{x} = \frac{\partial f}{\partial x} \dot{x} + \left[\frac{\partial g_1}{\partial x} \dot{x}, \frac{\partial g_2}{\partial x} \dot{x}, \dots, \frac{\partial g_n}{\partial x} \dot{x} \right] g^{-1}(x) [\dot{x} - f(x)] + \omega_i I [\dot{x}_d - \dot{x}] \quad (B 9)$$

Substituting for \dot{x}_d and rearranging the results as

$$\ddot{x} - \left(\frac{\partial f}{\partial x} - \omega_i I \right) \dot{x} + \omega_i \Omega (x - x_c) - \left[\frac{\partial g_1}{\partial x} \dot{x}, \frac{\partial g_2}{\partial x} \dot{x}, \dots, \frac{\partial g_n}{\partial x} \dot{x} \right] g^{-1}(x) [\dot{x} - f(x)] = 0 \quad (B 10)$$

Now, define $z_1 = x - x_c$. For constant x_c , $\dot{z}_1 = \dot{x}$. Then define $z_2 = \dot{x}$. A state-space system for $z = (z_1^T, z_2^T)^T$ is given by

$$\dot{z}_1 = z_2 \tag{B 11}$$

$$\dot{z}_2 = -\omega_i \Omega z_1 + \left(\frac{\partial f}{\partial x} - \omega_i I \right) z_2 + l(z)$$

$$\text{where } l(z) = \left[\frac{\partial g_1}{\partial x} z_2, \frac{\partial g_2}{\partial x} z_2, \dots, \frac{\partial g_n}{\partial x} z_2 \right] g^{-1}(x) [\dot{x} - f(x)]$$

Rewring Eqn B-11 as

$$\dot{z}_1 = z_2 \tag{B 12}$$

$$\epsilon \dot{z}_2 = -\Omega z_1 - z_2 + \epsilon \left(\frac{\partial f}{\partial x} z_2 + l(z) \right)$$

$$\text{where } \epsilon = \frac{1}{\omega_i}$$

On application of *Singular Perturbation Control* theory [\[34\]](#) to Eqn (B 12)

$$\bar{z}_2 = -\Omega \bar{z}_1 \text{ and } \dot{\bar{z}}_1 = -\Omega \bar{z}_1 \text{ which is exponentially stable for } \Omega > 0$$

Appendix C

Theory of Feedback Linearization

C.0 Single Input-Single Output(SISO) systems

A Single Input Single Output (SISO) affine control system obeys the following state and output relation [28], [35]

$$\begin{cases} \dot{x} = f(x) + g(x)u \\ y = h(x) \end{cases} \quad (C\ 1)$$

Where $x \in R^n$, $u \in R$, $y \in R$ and $f, g : R^n \rightarrow R^n$ are smooth vector fields and $h : R^n \rightarrow R$ is a smooth scalar function.

Differentiate output equation y with respect to time t along the trajectories of x

$$\begin{aligned} \dot{y} &= \frac{\partial h(x)}{\partial x} \dot{x} = \frac{\partial h}{\partial x} [f(x) + g(x)u] \\ &= \frac{\partial h}{\partial x} f(x) + \frac{\partial h}{\partial x} g(x)u = L_f h(x) + L_g h(x)u \end{aligned} \quad (C\ 2)$$

It is clear from the eqn C2, that there is no immediate change in y , if u is changed immediately and the change comes gradually via x . The \dot{y} directly depends on u , if and only if $L_g h(x) = \frac{\partial h}{\partial x} g(x) \neq 0$ and we will say that the relative degree of the system, $r = 1$.

Now, let us assume that $L_g h(x) = 0$ and differentiate output once again, we will get

$$\ddot{y} = L_f^2 h(x) + L_g L_f h(x)u \quad (C\ 3)$$

The system have said to relative degree, $r = 2$ if $L_g L_f h(x) \neq 0$. Repeat the process upto r derivatives, and we will say the relative degree is r . So r th derivative of output is as follows

$$y^{(r)} = L_f^r h(x) + L_g L_f^{r-1} h(x)u \quad (C\ 4)$$

Relative Degree :- The SISO system given by equation C.1 is said to have relative degree r at a point x^0 if

1. $L_g L_f^{r-1} h(x) = 0$; $k = 0, 1, 2, \dots, r-1$ for $\forall x$ in the neighbourhood of x^0

$$2. L_g L_f^{r-1} h(x) \neq 0$$

The following formula describing the time derivatives of the output is an immediate consequences of the definition of relative degree

$$\frac{d^k y}{dt^k} = y^{(k)} = \begin{cases} L_f^k h(x) & k = 0, 1, 2, \dots, r-1 \\ L_f^k h(x) + L_g L_f^{k-1} h(x) u & k = r \end{cases} \quad (C 5)$$

Remark:- For SISO linear system

$$\begin{cases} \dot{x} = Ax + Bu \\ y = Cx \end{cases} \quad (C 6)$$

The relative degree is the difference in degree between the numerator and denominator.

Equivalently, the relative degree of SISO, LTI system is the positive integer r , such that $L_g L_f^{r-1} h = C A^{r-1} B \neq 0$

Strong relative degree:- A system is said to have strong relative degree if the relative degree is r , for all $x^0 \in R^n$

C.0.1 Input-Output Linearization

Consider a system with a strong relative degree r . Then we have the r^{th} derivative of the output is given by

$$y^{(r)} = L_f^r h(x) + L_g L_f^{r-1} h(x) u$$

If v is a reference signal, such that $y^{(r)} = v$, therefore the feedback control law as

$$u = (L_g L_f^{r-1} h(x))^{-1} \{v - L_f^r h(x)\} \quad (C 7)$$

So, the resulting transfer function between v and y is given by

$$y(s) = \frac{1}{s^r} v(s) \quad (C 8)$$

Proposition:- Suppose a system of the form equation C.1 has relative degree r at a point x^0 . Define

$$z \triangleq \begin{pmatrix} z_1 \\ z_2 \\ \vdots \\ z_r \end{pmatrix} \triangleq \begin{pmatrix} \phi_1(x) \\ \phi_2(x) \\ \vdots \\ \phi_r(x) \end{pmatrix} \triangleq \begin{pmatrix} h(x) \\ L_f h(x) \\ \vdots \\ L_f^{r-1} h(x) \end{pmatrix}$$

and (C 9)

$$\eta \triangleq \begin{pmatrix} z_{r+1} \\ z_{r+2} \\ \vdots \\ z_n \end{pmatrix} \triangleq \begin{pmatrix} \phi_{r+1}(x) \\ \phi_{r+2}(x) \\ \vdots \\ \phi_n(x) \end{pmatrix}$$

The *Normal form* of a affine control system (Eqn C.1) is given by

$$\begin{aligned} \dot{z}_1 &= z_2 \\ \dot{z}_2 &= z_3 \\ &\vdots \\ \dot{z}_r &= b(z) + a(z)u \\ \dot{\eta} &= q(z, \eta) \end{aligned} \tag{C 10}$$

With output $y = z_1$

Notice that if we choose the feedback law

$$u = [a(z)]^{-1} \{v - b(z)\} \tag{C 11}$$

Then the resulting system from the reference input v to the output $y = z_1$ is linear.

Notice that the *Internal dynamics* / *Zero dynamics* $\dot{\eta} = q(z, \eta)$ are possibly non-linear, so the system is not been fully linearized by the feedback law

$$u = [a(z)]^{-1} \{v - \lambda_0 z_1 - \lambda_1 z_2 - \dots - \lambda_{r-1} z_r - b(z)\} \tag{C 12}$$

The resulting transfer funtion from input to output:

$$\frac{y(s)}{v(s)} = \frac{1}{\lambda_{r-1}s^r + \dots + \lambda_0} \tag{C 13}$$

C.1 Multi Input-Multi Output (MIMO) Systems

The concepts used in the SISO system such as Input-State Linearization, Input-Output Linearization, normal forms and zero dynamics and so on can be extended to MIMO systems. For the MIMO case, we consider the square systems i.e systems with same number of inputs as outputs.

$$\dot{x} = f(x) + \sum_{i=1}^{i=m} g_i(x) u_i$$

$$\begin{aligned}
y_1 &= h_1(x) \\
y_2 &= h_2(x) \\
&\vdots \\
y_m &= h_m(x)
\end{aligned} \tag{C 14}$$

Where the state vectors u_i 's ($i = 1, 2, \dots, m$) are control inputs, y_j 's ($j = 1, 2, \dots, m$) are outputs, f & g_i 's are smooth vector fields and h_j 's are smooth scalar functions. If we collect the control inputs u_i 's into vector u , corresponding vectors into matrix G , and the outputs into vector y , then the system equations can be written collectively as

$$\begin{aligned}
\dot{x} &= f(x) + G(x)u \\
y &= h(x)
\end{aligned} \tag{C 15}$$

C 1.1 Feedback Linearization of MIMO systems

The approach to obtain the I/O linearization of MIMO systems is again to differentiate the outputs y_j 's of the system until the inputs appear, similarly to the SISO case. The output differentiations can be written compactly as follows

$$\begin{bmatrix} y_1^{(r_1)} \\ y_2^{(r_2)} \\ \vdots \\ y_m^{(r_m)} \end{bmatrix} = \begin{bmatrix} L_f^{r_1} h_1 \\ L_f^{r_2} h_2 \\ \vdots \\ L_f^{r_m} h_m \end{bmatrix} + E(x) \begin{bmatrix} u_1 \\ u_2 \\ \vdots \\ u_m \end{bmatrix} \tag{C 16}$$

Where the $m \times m$ matrix $E(x)$ is defined as

$$E(x) = \begin{bmatrix} L_{g_1} L_f^{r_1-1} h_1 & L_{g_2} L_f^{r_1-1} h_1 & \cdots & \cdots & L_{g_m} L_f^{r_1-1} h_1 \\ L_{g_1} L_f^{r_1-1} h_2 & L_{g_2} L_f^{r_1-1} h_2 & \cdots & \cdots & L_{g_m} L_f^{r_1-1} h_2 \\ \vdots & \vdots & \vdots & \vdots & \vdots \\ \vdots & \vdots & \vdots & \vdots & \vdots \\ L_{g_1} L_f^{r_1-1} h_m & L_{g_2} L_f^{r_1-1} h_m & \cdots & \cdots & L_{g_m} L_f^{r_1-1} h_m \end{bmatrix} \tag{C 17}$$

The matrix $E(x)$ is called the *Decoupling matrix* for the MIMO system. If the decoupling matrix is non-singular in a region Ω around a point x^0 , the the input transformation

$$u = -E^{-1}(x) \begin{bmatrix} L_f^{r_1} h_1 \\ L_f^{r_2} h_2 \\ \vdots \\ L_f^{r_m} h_m \end{bmatrix} + E^{-1}(x) \begin{bmatrix} v_1 \\ v_2 \\ \vdots \\ v_m \end{bmatrix} \quad (C 18)$$

yields a linear differential relation between the output y and the new input v as

$$\begin{bmatrix} y_1^{(r_1)} \\ y_2^{(r_2)} \\ \vdots \\ y_m^{(r_m)} \end{bmatrix} = \begin{bmatrix} v_1 \\ v_2 \\ \vdots \\ v_m \end{bmatrix} \quad (C 19)$$

Note that the above Input-Output relation is decoupled , in addition to being linear. Since only affects the corresponding the output y_j , but not the others , a control of the form (C.17) is called a *decoupling control law or non-interacting control law*.

Bibliography

- [1] Aranya Chakraborty and Murat Arcak. A Two-Time-Scale Redesign for Robust Stabilization and Performance Recovery of Uncertain Nonlinear Systems. *Proceedings of the 2007 American Control Conference, New York City, USA, July 11-13, 2007*.
- [2] Radhakant Padhi et al. Nonlinear and Linear Autopilot Performance Comparison of Tactical Flight Vehicle. *AIAA Guidance, Navigation and Control Conference and Exhibit 2012*.
- [3] Bin Jiang, Jian Liang Wang et al. An Adaptive Technique for Robust diagnosis of faults with independent effects on system outputs. *Int.J. Control*, 2002. Vol 75, No. 11, 792-802.
- [4] Xiadong Zhang, Thomas Parisini and Marios M. Polycarpou. Adaptive Fault-Tolerant Control of Nonlinear Uncertain Systems: An Information-Based Design Approach. *IEEE Transactions on Automatic Control*, Vol.49, No.8, August 2004.
- [5] J Marzat, H Piet-Lahanier et al. Model-Based fault diagnosis for aerospace systems: a survey. *Proceedings of the Institution of Mechanical Engineers, Part G: Journal of Aerospace Engineering*, Jan 2012.
- [6] Jinhua Fan, Youmin Zhang and Zhiqiang Zheng. Adaptive Observer-Based Integrated Fault Diagnosis and Fault-Tolerant Control Systems Against Actuator Faults and Saturation. *Journal of Dynamic Systems, Measurement, and Control*, July 2013, Vol.135/ 041008-1.
- [7] Missile Flight Simulation, Part-1, Surface-to-Air Missiles. *MIL-HDBK-1211*, 17 July 1995.
- [8] Michel B. McFarland and Shaheen M. Hoque. Robustness of a Nonlinear Missile Autopilot Designed using Dynamic Inversion. *AIAA Guidance, Navigation and Control Conference and Exhibit 14-17 August 2000, Paper No. AIAA-2000-3970*.
- [9] Corey J. Schumacher, Pramod P. Khargonekar et al. Stability Analysis of Dynamic Inversion Controllers using Time-Scale Separation. *American Institute of Aeronautics and Astronautics, Inc 1998, Paper No. AIAA-98-4322*.
- [10] S.E. Talole, A.A. Godbole et al. Robust Roll Autopilot Design for Tactical Missiles. *Journal of Guidance, Control, and Dynamics*, Vol.34, No.1, January-February 2011.

- [11] Corey J.Schumacher and Pramod P.Khargonekar. Stability Analysis of Missile Control System with a Dynamic Inversion Controller. *Journal of Guidance, Control, and Dynamics*, Vol.21, No.3, May-June 1998.
- [12] Ranajit Das, Abhijit Das et al. Nonlinear Design of Three Axis Autopilot for a tactical Aerospace Vehicle . *International Symposium on Industrial Electronics, ISIE-2006, July 9-13, Montreal, Canada*.
- [13] P.N. Dwivedi, A.Bhattacharya et al. Nonlinear Autopilot Design Via Sliding Mode: Two Different Approaches. *American Institute of Aeronautics and Astronautics*.
- [14] Ming Xin and S.N. Balakrishnan et al. Nonlinear Missile Autopilot Design with $\theta - D$ technique. *Anteon corporation granted paper for study of Naval Surface Warfare*.
- [15] P.K.Menon and V.R.Iragavarapu . Nonlinear Missile Autopilot Design using Time-Scale separation. *American Institute of Aeronautics and Astronautics, Paper No. AIAA-97-3765*.
- [16] Qian Wang, Robert F.Stengel. Robust Control of Nonlinear Systems with Parametric Uncertainty. *Automatica* 38 (2002) 1591-1599.
- [17] Zarchan P. Tactical and Strategic Missile Guidance. *AIAA Inc., Fourth edition, 2002*.
- [18] Harkegard O. Backstepping and Control Allocation with Applications to Flight Control. *PhD thesis, Department of Electrical Engineering, Linkoping University , SE-58183,Linkoping, Sweden, April 2003*.
- [19] Mracek C P and Ridgely D B. Missile Longitudinal Autopilots: Comparision of Multiple Three Loop Topologies. *Paper No. AIAA-2005-6380-CP, Proceedings of AIAA GNC Conference and Exhibit at San Francisco, California, 2005*.
- [20] Devaud E, Harcaut J P, and Siguerdidjane H. Various Strategies To Design A Three-Axis Missile Autopilot. *Paper No. AIAA-99-3976-CP, 1999*.
- [21] Font S. Devaud E., Siguerdidjane H. Nonlinear dynamic autopilot design for the nonminimum phase missile. *37 th IEEE conference on decision and control*
- [22] Siguerdidjane H., Devaud E. and Harcaut J.P. Some control strategies of high angle-of-attack missile autopilot. *14 th IFAC symposium on Automatic control in Aerospace*
- [23] Siguerdidjane H., Devaud E. and Harcaut J.P. Three axis missile autopilot design: From linear to Nonlinear strategies. *Journal of Guidance, Control, and Dynamics*

- [24] Kar P K, Sarkar A K et al. Aerodynamic Coefficients Estimation of a Flight Vehicle from different flight trails under limited measurements. *Paper No. AIAA-2011-6274-CP, Proceedings of AIAA Atmospheric Flight Mechanics Conference and Exhibit, Portland, Oregon, (8-11) August 2011.*
- [25] Stengel R F. Flight Dynamics. *Princeton University Press, New Jersey, First edition 2004.*
- [26] Lin C F. Advanced Control System Design. *American GNC Corporation, PTR Prentice Hall, New Jersey, First edition 1993.*
- [27] Lee T and Kim Y. Nonlinear Adaptive Flight Control using Backstepping and Neural Networks Controller. *Journal of Guidance, Control, and Dynamics, 24(4): 107-117, July 2001.*
- [28] Slotine J E and Li Weiping. Applied Nonlinear Control. *Prentice Hall International Inc. First edition, 1991.*
- [29] Robert C Nelson. Flight Stability and Automatic Control. *Mc-Graw Hill International editions, Second edition, 1998.*
- [30] George M. Siouris. Missile Guidance and Control Systems. *Springer-Verlag, New York Inc, 2004 edition.*
- [31] Michael V Cook. Flight Dynamics Principles. *Second edition, 2007.*
- [32] Hassan Nora, Didier Theilliol et al. Fault-tolerant Control Systems: Design and Practical Applications. *Springer-Verlag, London Limited, 2009.*
- [33] George P Sutton. Rocket Propulsion Elements. *John-Wiley& Sons Inc. Seventh edition, 2001.*
- [34] Peter Kokotovic, Hassan K Khalil, John O'Reilly. Singular Perturbation Methods in Control. *SIAM edition, Academic Press London, 1996.*
- [35] Hassan K Khalil. Nonlinear Systems. *Prentis Hall, Third edition.*
- [36] Schumacher C. and Khargonekar P.P. Missile Autopilot designs using H_∞ control with gain scheduling and dynamic inversion. *Journal of Guidance, Control, and Dynamics*
- [37] William L., Snel S.A., Enns D.F and Garrard Jr. Nonlinear inversion flight control for a super maneuverable aircraft. *Journal of Guidance, Control, and Dynamics, 15.*
- [38] Tahk M., Menon P.K. and Briggs M. Application of plant inversion via state feedback to missile autopilot design. *IEEE transaction, Conference of Decision and Control, 27 th proceedings.*

- [39] Lawrence D.A and Rugh W.J. Gain Scheduling dynamic linear controllers for a nonlinear plant. *Proceedings of 32 nd IEEE conference on Decision and Control*.
- [40] Jason G.W. David P.W. and Douglas A.L. Missile Autopilot design using a gain scheduling technique. *IEEE transaction*.
- [41] Kargonekar P.P., Kamener I., Pascol A.M., Coleman E.E. Velocity algorithm for implementation of gain scheduled controllers. *Automatica*, 31.
- [42] Powly A.A. and Bhat M.S. Missile Autopilot design using discrete time variable structure controller with sliding sector. *Journal of Guidance, Control, and Dynamics*, 27.
- [43] Zak S.H. Decarlo R.A. and Mathews G.P. Variable structure control of nonlinear multivariable systems: A tutorial. *Proceedings of IEEE*, 76.
- [44] Leonhardt B.K., Rysdyk R.T. and Calise A.J. Development of intelligent flight propulsion and control system: Nonlinear Adaptive control. *AIAA Guidance, Navigation and Control Conference and Exhibit*.
- [45] Jeff S. Shamma. and James R. Cloutier. Gain scheduled missile autopilot design using Linear Parameter Varying transformations. *Journal of Guidance, Control, and Dynamics*, 16(2): 256-263, March-April, 1993.
- [46] J.J. Zhu and M.C. Mickle. Missile Autopilot design using the Extended Mean Assignment control and stabilization. *Proceedings of the 27 th southeastern Symposium on system theory*, pages 247-251, 12-14, March 1995.
- [47] J.J. Zhu and M.C. Mickle. Missile Autopilot design using the Extended Mean Assignment control and stabilization. *Proceedings of the 27 th southeastern Symposium on system theory*, pages 120-124, March 1996.
- [48] Steinicke A. and Michalka G. Improving transient performance of dynamic inversion missile autopilot by using backstepping. *AIAA Guidance, Navigation and Control Conference and Exhibit*.
- [49] Goshal T.K. and Das G. Structured design methodology of missile autopilot. *IE (I) Journal-AS*, 76.
- [50] Rugh W.J. and Jackson P.B. Analysis of gain scheduling for the three-loop autopilot structure. *Applied physics Lab, Johns Hopkins University*.
- [51] Greensite L. Analysis and Design of Space Vehicle Flight Control system. *Pergamon press, Second edition, Oxford, 1980*.